2010-03-27

Regional Mechanical Function Changes Remain after Ventricular Pacing Cessation: Evidence of Mechanical Cardiac Memory

Jeremy Kenneth Skorinko
Worcester Polytechnic Institute

Regional Mechanical Function Changes Remain after Ventricular Pacing Cessation: Evidence of Mechanical Cardiac Memory

A thesis to be submitted to the faculty of Worcester Polytechnic Institute in partial fulfillment of the requirements for the Degree of Master of Science

Submitted by:

Jeremy Kenneth Skorinko
Biomedical Engineering

Approved by:

Glenn R. Gaudette, PhD
Assistant Professor
Worcester Polytechnic Institute
Department of Biomedical Engineering

Kristen L. Billiar, PhD
Associate Professor
Worcester Polytechnic Institute
Department of Biomedical Engineering

Ki H. Chon, PhD
Professor
Worcester Polytechnic Institute
Department of Biomedical Engineering

Acknowledgements

Many thanks to my committee members: Kristen Billiar, and Ki Chon for their direction and support also, for their continued guidance to further my education.

I would also like to thank Jacques Guyette for his help in collecting the data for this project.

I would like to thank my entire family for their support and encouragement.

Finally, I would like to thank my advisor Glenn Gaudette for the countless hours he has spent guiding me through this project and for all of the support he has given when it was most needed.

Abstract

Every year 400,000 – 600,000 people in the United States die from sudden cardiac death. Sudden cardiac death is often caused by irregular electrical impulses, or arrhythmias, in the heart. Arrhythmias can be corrected through pharmacological therapies, device therapies, or both. One type of device therapy, pacemakers, are inserted in the heart to correct arrhythmias. After a period of ventricular pacing, cardiac memory is defined by changes in the T-wave that are persistent upon return to normal activation pathways. During ventricular pacing, regional stroke work in areas closest to the pacing electrode is significantly decreased. We hypothesize that the mechanical function in the region around the pacing site will continue to have altered mechanical function after cession of pacing, in effect showing a mechanical cardiac memory.

To test the hypothesis, nine canine models were implanted with pacing electrodes in both the atrium and ventricle. After a forty-minute stabilization period, baseline data were obtained during atrial pacing. Cardiac memory was induced in five canine models through a two-hour period of ventricular pacing followed immediately by atrial pacing. The remaining canine models served as controls, undergoing atrial pacing for two hours. High-density mapper (HDM) was used to determine mechanical function in a region centered approximately 1 cm away from the pacing electrode.

No differences in global function (tau, developed pressure, dP/dt_{max}, dP/dt_{min}) were found after two hours of ventricular pacing upon return to normal activation pathways. There was a significant decrease in regional stroke work in an area close to the electrode between baseline (5.7 ± 2.6 %), during ventricular pacing (-3.8 ± 0.9 %)($p<0.05$) and after two hours of ventricular pacing upon return to normal activation pathways (2.4 ± 1.6 %)($p<0.05$). Further, systolic area contraction was also significantly different between baseline (5.0 ± 6.6 %) and after two hours of ventricular pacing upon return to normal activation pathways (0.2 ± 7.4 %)($p<0.05$). Diastolic twist and diastolic twist rates showed no significant differences. Finally, contractile principal strain increased by inducing cardiac memory (-2.6 ± 0.3 %) as compared to baseline (-1.1 ± 0.5 %)($p<0.05$). These findings suggest there is a mechanical correlation to electrical cardiac memory.

Table of Contents

Acknowledgements **2**

Abstract **3**

1 Introduction **8**

2 Background **11**
2.1 Normal Heart Rhythm **11**
2.2 Arrhythmias **15**
2.3 Cardiac Mechanics **17**
2.3.1 Global Cardiac Mechanics 17
2.3.2 Regional Cardiac Mechanics 20
2.4 High Density Mapper **25**
2.4.1 Image Processing 25
2.4.2 Post-processing of data 27
2.5 Pacing **28**
2.6 Cardiac Memory **30**
2.6.1 Short-term Cardiac Memory 32
2.6.2 Long-term Cardiac Memory 33

3 Hypothesis and Specific Aims **37**
3.1 Hypothesis **37**
3.2 Specific Aim 1 ..... **37**
3.3 Specific Aim 2 ..... **38**

4 Materials and Methods **39**
4.1 Animal Surgery **39**
4.2 Pacing **39**
4.3 Data Acquisition **41**
4.4 Global Function **42**
4.5 Specific Aim 1: Mechanical Analysis **43**
4.6 Specific Aim 2: Diastolic Twist **46**
4.7 Specific Aim 2: Systolic Principal Strain **48**
4.8 Statistics **50**

5 Results **52**
5.1 Global Function **52**
5.2 Specific Aim 1: Mechanical Correlation to Cardiac Memory **52**
5.3 Specific Aim 2: Diastolic Twist **61**
5.4 Specific Aim 2: Systolic Principal Strain **61**

6 Discussion **64**
6.1 Global Function **64**
6.2 Ventricular Pacing **65**
6.3 Specific Aim 1: Mechanical Correlation to Cardiac Memory **66**
6.4 Specific Aim 2: Diastolic Twist **68**
6.5 Specific Aim 2: Systolic Principal Strain **68**

7 Conclusions **71**

8 Future Studies **72**

Table of Figures

Figure 2.1: Action Potentials **12**

Figure 2.2: Left ventricular pressure versus volume work loop **19**

Figure 2.3: Determination of Tau **19**

Figure 2.4: Graphical representation of strain **22**

Figure 2.5: Mohr's Circle **23**

Figure 2.6: Example of region of interest in HDM **28**

Figure 2.7: Electrocardiogram with inverted T-Wave **32**

Figure 4.1: Pacing electrode locations **40**

Figure 4.2: Pacing protocol timeline **40**

Figure 4.3: Determination of scale by pixels per centimeter **41**

Figure 4.4: Tau is the exponential fit to the pressure (mmHg) versus time (s) during isovolumic relaxation **43**

Figure 4.5: Discrete integration of work loop leads to regional stroke work **45**

Figure 4.6: Determination of systolic area contraction **45**

Figure 4.7: Region of interest with a single sub-region highlighted **46**

Figure 4.8: 2-D coordinate system of the camera is denoted with X'Y' where the cylindrical cardiac axes are denoted with ZRϕ **48**

Figure 4.9: Graphical depiction of principal strains **50**

Figure 5.1: Regional stroke work vs. time **54**

Figure 5.2: Representitive work loops **55**

Figure 5.3: Systolic area contraction vs. time **57**

Figure 5.4: sub-regions of interest **58**

Figure 5.5: A) regional stroke work gradients **59**

Figure 5.6: Scatter plot of regional stroke work vs. distance from pacing electrode **60**

Table of Tables

Table 2-1: Intracellular and Extracellular Ion Concentrations and Equilibrium Potentials in Cardiac Muscle Cells 12

Table 2-2: Major currents during ventricular action potential including protein subunit and the phase involvement 14

Table 5-1: Global function results show no difference in any parameter measured between baseline and 2 hours of pacing. Data: mean ± SEM..... 52

Table 5-2: Diastolic twist and diastolic twist rate in Cardiac memory animals at baseline (t=0), during ventricular pacing, and after 2 hours of ventricular pacing upon return to normal activation. Data: Mean ± SEM 61

Table 5-3: Control animal systolic principal strains at baseline (t=0) and after 2 hours of atrial pacing. Data: Mean ± SEM 62

Table 5-4: Cardiac memory animal systolic principal strain results at baseline (t=0), during ventricular pacing, and after 2 hours of ventricular pacing upon return to normal activation pathways. Data: Mean ± SEM 63

1 Introduction

There are several pathologies that affect the normal rhythm of the heart. Of these, arrhythmias are the most common and can occur in both the atria and the ventricle. Arrhythmias often can be corrected using pharmacological therapies or device therapies. Pharmacological therapies aim to correct the flow of ions across the myocyte membrane. While in many cases it is sufficient, often it is necessary to use device therapy to treat underlying pathology. When a specific region in the heart is causing an arrhythmia it can often be corrected by ablation (kills or isolates problematic area). When there is no specific area causing the arrhythmia it is often necessary to use cardiac pacing that alters activation pathways in the heart and can lead to changes in the myocardial structure. Understanding the underlying mechanisms responsible for these changes in myocardial structure from device therapy may improve effectiveness of pharmacological therapies.

Despite advances in cardiac devices and pharmacological therapies, each year 400,000 - 600,000 people in the US die from sudden cardiac death[1]. Sudden cardiac death may occur when the electrical impulses in the heart become more rapid, as in ventricular tachycardia, or chaotic, as in ventricular fibrillation. These arrhythmias referred to as irregular heartbeats lead to decreases in cardiac output (amount of blood pumped out of the heart).

Normal electrical activation in the heart begins in the sinoatrial node and propagates through the atrium to the atrioventricular node where it travels through the

Bundle of His then both bundle branches to the purkinje fibers. Pacing electrodes stimulate the heart from the point of insertion. Pacing from the atrium has little or no effect on the mechanical function or work done by the ventricle. Inserting electrodes in the ventricle wall and pacing from there alters normal activation pathways, which decreases mechanical function and globally decreases work[2]. In the ventricle the pacing electrode creates a gradient of regional stroke work with the least work done near the pacing site. In addition the regional stroke work increases with distance from the pacing location[3].

Ventricular pacing induces an electrophysiological change as seen in electrocardiograms as a change in the T-wave called cardiac memory. Cardiac memory is defined by an altered T-wave induced by ventricular pacing or other arrhythmic events that persists for variable lengths of time after return to normal activation pathways. Chatterjee et al.[4] were the first to report altered T-waves due to ventricular pacing. The term "cardiac memory" was coined by Rosenbaum et al.[5] after studying ventricular pacing, more specifically, the time period following ventricular pacing when normal activation pathways were resumed with respect to T wave changes[5]. Current research provides much deeper insights as to the possible reasons for cardiac memory from a molecular sense[6]. Also, two types of cardiac memory have been shown: short-term (STCM) and long-term (LTCM). Short-term cardiac memory has been induced after just two hours of ventricular pacing and lasts for a period of time proportional to the pacing time, whereas long-term cardiac memory has been induced after seven days of pacing with a return to control levels as a function of the time paced[7].

Cardiac memory is determined during the time period that follows cessation of abnormal activation. It has been shown that 21 - 25 days of pacing invokes steady state T-wave changes for two days that return to control levels by seven days. Pacing for 42 - 52 days invokes steady state T-wave changes for four to five days that do not return to control levels after 30 days of observation[8]. While mechanical function has been investigated during ventricular pacing extensively[2, 3, 9, 10], changes that remain after cessation of pacing have not been studied at length. Herein we will determine if any mechanical function changes remain after inducing cardiac memory. These data might provide important clues for all mechanisms involved in cardiac memory.

2 Background

2.1 Normal Heart Rhythm

An action potential is an electrochemical activity that allows different cells to carry a signal over a distance; the most notable is skeletal muscle, however cardiac muscle cells are also excitable by action potentials. Cardiac myocytes are similar to skeletal muscle because the resting membrane potential is negative[11]. Myocytes are striated and have the same contractile apparatus as skeletal muscle cells. Unlike skeletal muscle that receives stimulation from nerve cells, the heart beats on it own because of specialized cells in the sinoatrial (SA) node, called pacemaker cells, and specialized tissue in the atrioventricular (AV) node that conducts the impulses from atria to ventricles[12]. The nodal cells undergo a slow response action potential (Figure 2.1A), where the influx of ions increases the voltage difference between the extracellular space and intracellular space past the stimulation potential. Ventricular and atrial myocytes undergo a fast response action potential (Figure 2.1 B). The slow and fast action potentials differ from each other in shape, height, and duration. The fast action potential's resting membrane potential (-90mV) is considerably more negative than that of the slow action potential (-60mV). The fast action potential has a rapid upstroke followed by an overshoot with a "notch" and then a plateau and finally a repolarization, while the slow action potential has a slower upstroke with no "notch" followed by a plateau and a slower repolarization.

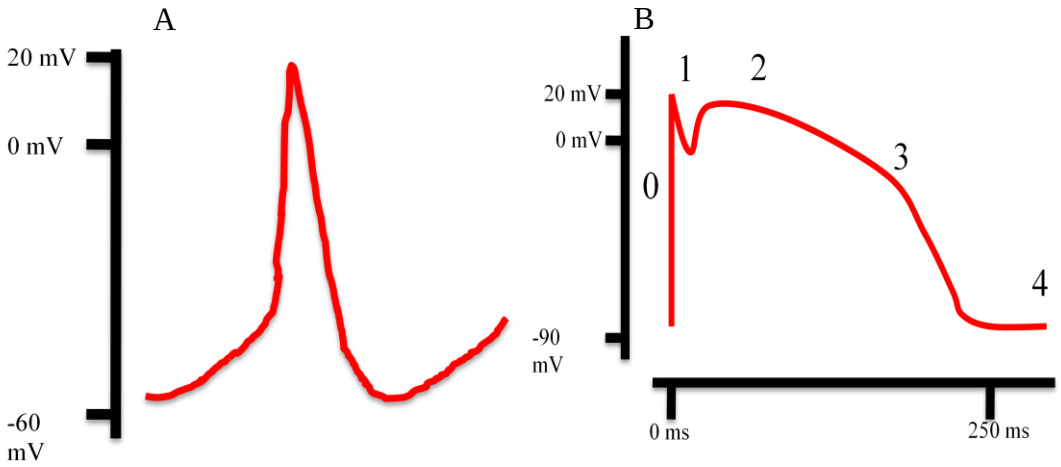

Figure 2.1: A) Example of a slow action potential B) Example of a fast action potential with phases labeled (0: Rapid Upstroke 1: Knotch 2: Plateau 3: Repolarization 4: Resting Membrane Potential)

There are three main ions that produce action potentials in the heart, Na^+, K^+, and Ca^{2+}. Table 2-1 shows the intracellular and extracellular concentrations at equilibrium in the heart[12]. Altering the conductance of the membrane to different ions allows for passage of these ions across the cell membrane. The resulting changes in intracellular ion concentrations change the membrane potential.

Table 2-1: Intracellular and extracellular ion concentrations and equilibrium potentials in cardiac muscle cells

Ion	Extracellular Concentrations (mM)	Intracellular Concentrations (mM)	Equilibrium Potential (mV)
Na^+	145	10	70
K^+	4	135	-94
Ca^{2+}	1.4	0.1	132

There are five phases to the ventricular action potential as shown in Figure 2.1. Phase 4 is the resting membrane potential; this is the period that the cell remains in

until it is stimulated by an external stimulus, typically an adjacent cell. Phase 0 is the rapid depolarization phase. This phase is due to the opening of the fast Na^+ channels causing a rapid increase in Na^+ membrane conductance (G_{Na}) and a rapid influx of Na^+ ions cell resulting in a Na^+ current (I_{Na}). Phase 1 of the action potential occurs with the inactivation of the Na^+ channels and the opening of the outward K^+ currents (I_{to1}, I_{to2}) that contribute to the "notch" of some ventricular myocyte action potentials, particularly I_{to2}, this drives the action potential back down. Phase 2 is the plateau phase of the cardiac action potential where the membrane voltage is essentially zero. A balance between the outward K^+ current and the inward Ca^{2+} current (I_{Ca}) maintains the plateau. Finally, Phase 3 is the rapid repolarization phase of the action potential. This occurs when the Ca^{2+} channels close and the K^+ channels remain open to ensure a net outward current bringing the myocyte back to its resting membrane potential. Table 2-2 shows the major ions and ion currents that affect the cardiac action potential along with the protein subunits and the phase of the action potential or the role that the current plays in ion transfer. These currents help to increase the membrane potential past its threshold so the action potential fires making the cardiac cell beat and propagate its signal to the next cell[11].

Table 2-2: Major currents during ventricular action potential including protein subunit and the phase involvement

Ion	Current	α subunit protein	Phase/role
Na^+	I_{Na}	$Na_V1.5$	0
Ca^{2+}	$I_{Ca(L)}$	$Ca_V1.2$	0-2
K^+	I_{to1}	$K_V4.2/4.3$	1, Notch
K^+	I_{Ks}	$K_V7.1$	2,3
K^+	I_{Kr}	$K_V11.1$ (hERG)	3
K^+	I_{K1}	$K_{ir}2.1/2.2/2.3$	3,4
Na^+, Ca^{2+}	I_{NaCa}	$3Na^+$-$1Ca^{2+}$-exchanger	Ion Homeostasis
Na^+, K^+	I_{NaK}	$3Na^+$-$2K^+$-ATPase	Ion Homeostasis
Ca^{2+}	I_{pCa}	Ca^{2+}-transporting ATPase	Ion Homeostasis

Propagation from cell to cell occurs through specialized areas in the myocytes, called gap junctions, that directly connect the cytoplasm of the neighboring cells to allow for the flow of small molecules and ions. Gap junctions are the functional element responsible for the electrical propagation between myocytes allowing for the rapid contraction of the heart.

Optimal concentrations of sodium, potassium and calcium, are necessary in order for the heart to function correctly. Sodium is necessary for depolarization, whereas potassium can increase or decrease the duration of the action potential. Calcium is essential for contraction of the myocyte. Decreasing the extracellular concentration

of calcium will decrease the contractility of the myocardium, whereas increasing the extracellular concentration of calcium will increase contractility (within limits). The intracellular concentration of calcium is ultimately responsible for contraction. During the plateau phase of the action potential calcium permeability of the sarcolemma increases because voltage-gated calcium channels are opened. Once in the cytosol the calcium stimulates the opening of calcium release channels in the sarcoplasmic reticulum. The calcium in the cytoplasm binds to troponin C causing the movement of tropomyosin away from the myosin-binding sites and stimulating contraction. Relaxation of the ventricular myocyte is dependent on ATP-energized calcium pumps in the sarcoplasmic reticulum that are regulated by phospholamban. When phospholamban is phosphorlized its inhibition of the calcium pump is relieved allowing phosphorlation of troponin I that inhibits the binding of calcium to troponin C. This permits the tropomyocin to re-block the binding sites between actin and myocin filaments, thus relaxation occurs[12].

The flow of ions across the cell membrane will alter the flow of Ca^{2+} and hence affect mechanical contraction in the myocyte. Understanding how the ions and ion currents affect the action potential of the myocyte or the sinus rhythm of the heart is essential to determining the best therapy to correcting arrhythmias while minimizing the effect on mechanical function.

2.2 Arrhythmias

There are several pathologies of the heart that affect the action potential and therefore the sinus rhythm of the myocardium. Arrhythmias affect more than 3

million Americans yearly at a cost of $3.1 billion. The most common arrhythmia is atrial fibrillation, which affects 2.2 million Americans[1]. Atrial fibrillation is a fast and irregular rhythm in the atria, it can be a singular event or permanent reoccurrences can exist. Atrial flutters are similar to atrial fibrillations except they cause a fast and regular beat in the atria. Both of these conditions can cause blood clots to form in the atria because the blood does not flow correctly into the ventricle. Another condition called paroxysmal supraventricular tachycardia (PSVT) occurs when there is a problem with the electrical stimulus in the atria causing it to beat faster than normal. PSVT is an occasional pathology and is similar to atrial fibrillation. Atrial flutter is a type of PSVT. Atrial arrhythmias can be corrected with pharmacological therapies or ablation of the problematic area. If the problematic area is the sino-atrial node, a pacemaker will need to be implanted after ablation to regulate the heartbeat.

The ventricle can also experience arrhythmias. Ventricular tachycardia and bradycardia are the rapid beating (>100 beats per minute) of the ventricle and the slowed beating of the ventricle (<60 beats per minute), respectively, during periods of rest. Both of these pathologies decrease quality of life for the patient experiencing them. Ventricular tachycardia is caused when an area of the ventricle emits an action potential that propagates through the ventricle separate from sinus rhythm. Ventricular tachycardia is sometimes associated with atrial fibrillation where the rapid and chaotic firing in the atria is transmitted to the ventricle but some beats are blocked by the atrio-ventricular node making the rate in the ventricle slower than that in the atria. Tachycardia results in decreased blood flow to the body, including the

heart, because the increased rate reduces cardiac output by decreasing the stroke volume. Conversely, bradycardia can be caused by heart block or branch bundle block. Both heart block and bundle branch blocks are disruptions of the activation pathways to the ventricle where the pacing signal does not propagate from the atrium to the ventricle. Bradycardia also decreases cardiac output by the depressed heart rate.

Arrhythmias change the contraction of the myocardium by interrupting the normal electrical activation sequence. The contraction of the myocardium provides the pressure needed to circulate the blood through the body.

2.3 Cardiac Mechanics

2.3.1 Global Cardiac Mechanics

There are several measures of the function of the heart as a whole. As the left ventricle supplies blood throughout the body it performs more work than the right ventricle and is thicker, therefore most cardiac measurements focus on left ventricular function. Measurements include stroke volume, stroke work, ejection fraction, the isovolumic relaxation time constant, maximum change in left ventricular pressure over time, and minimum change in left ventricular pressure over time. Stroke volume is the amount of blood the heart is able to pump in beat and can be determined by Equation 1. Stroke volume is also a measure of the contractility of the heart however it is limited by heart rate[12].

$$SV = EDV - ESV \quad (1)$$

Integrating stroke volume with respect to left ventricular pressure produces stroke work (Equation 2). Stroke work is the amount of work done to eject blood from the ventricle to the aorta[12]. It is the amount of energy required to increase the pressure in the left ventricle higher than that in the aorta in order to eject the blood. The amount of blood ejected during one beat is measured by ejection fraction. Ejection fraction is the percentage of blood ejected from the ventricle in one beat (Equation 3). Both stroke volume and stroke work are measures of systolic function (Figure 2.2). Diastolic function is also important to the relaxation of the heart where stiffness and wall thickness can contribute to the function.

$$SW = \int SV \cdot dP \tag{2}$$

$$Ef = \frac{Volume_{EndDiastole} - Volume_{EndSystole}}{Volume_{EndDiastole}} \tag{3}$$

Isovolumic relaxation constant, tau, was determined by Weiss et al.[13] by assessing left ventricular pressure fall during isovolumic beats. They found left ventricular pressure fall dP/dt was exponential during isovolumic relaxation and thus can be characterized by a time constant tau (Equation 4) (Figure 2.3).

$$P = P_0 + e^{\frac{-t}{\tau}} \tag{4}$$

Clinically global function is measured by echocardiogram.

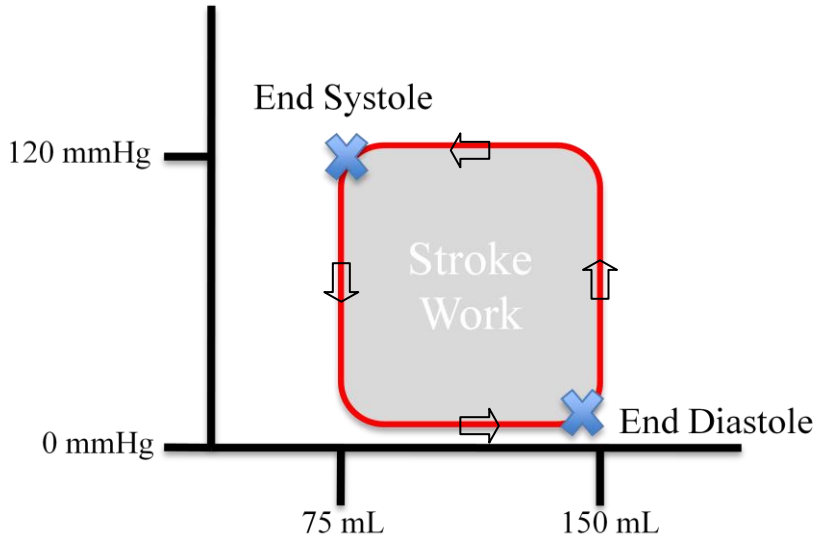

Figure 2.2: Left ventricular pressure versus volume work loop direction is counter clockwise. Gray area inside of loop is stroke work and is found by integration. Stroke volume is found by subtracting the end systolic volume from the end diastolic volume. Ejection fraction is found by dividing the stroke work by the end diastolic volume.

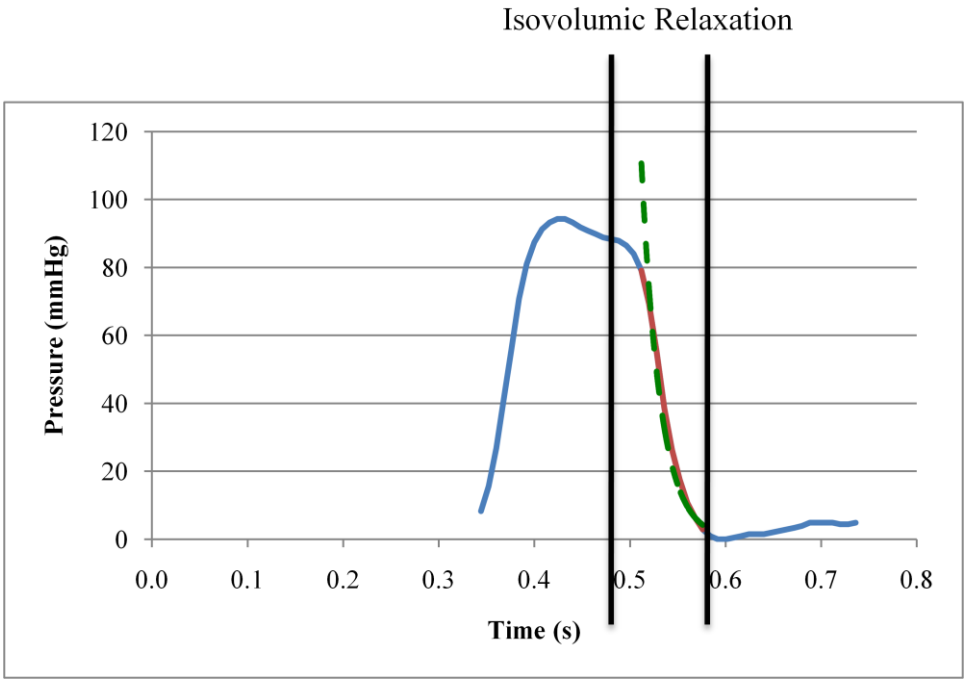

Figure 2.3: Determination of Tau. Green line is exponential fit to pressure vs. time during isovolumic relaxation. Black vertical lines delimit isovolumic relaxation

2.3.2 Regional Cardiac Mechanics

Different pathologies affect different regions of the heart; therefore there is a need to determine the mechanical function of the heart in many regions. Clinically, these measurements can be taken with several techniques. Magnetic resonance imaging (MRI) has become very popular in the last few decades. Tagged MRI is a method that can noninvasively measure the internal motions within the heart wall[14, 15]. This method uses locally induced perturbations of the magnetization to mark the myocardium. The deformation of these markers is the cue providing mechanical meaning to these functions. Marks will last for times on the order of one cardiac cycle. They will create a visible mark on the MR image that will move precisely with the underlying tissue. Therefore, the tagged MRI can be used to simultaneously measure motion of different regions of the heart. Tagged MRI is advantageous because it can measure the heart in 3-D, in addition to determining stroke volume and stroke work. It can also be used for local strain measurements to determine function in regions of the myocardium that may be damaged from ischemia[16, 17], hypertrophy[18], or infarction[19].

Echocardiograms (ECHO) are a non-invasive procedure for measuring the mechanical function of the heart; they use sound waves to determine the location of the heart wall during the cardiac cycle. It is one of the most widely used diagnostic tools for the heart. Using measurements from ECHO the size of the ventricular cavity can be measured in both the relaxed and contracted states to determine stroke volume (with the assumption the ventricle is a ellipsoid), from this ejection fraction and cardiac output are determined. ECHO is used to determine regional changes in wall

size, wall movements, wall stiffness, or cavity size. ECHO has been used most recently to determine strain and strain rate (discussed below) in the myocardium. ECHO measures tissue velocity that gives displacement when integrated over time. More recently a new method of ECHO has been employed called ultrasound speckle tracking imaging (STI). STI uses B-scan ultrasound to give the appearance of speckle patterns within the tissue, then motion analysis is done on the speckles to determine strain and ventricular torsion[20] .

Torsion is the twisting of the heart due to an applied force in the circumferential direction. Torsion can be measured during diastole. This measurement of torsion is a correlative of the isovolumic diastolic relaxation time constant (Tau)[21]. Dong et al. [21] used tagged MRI on canine models to measure the angle displacement of the base of the heart relative to the apex. These displacement angles were then transformed into torsion measurements and were compared to the curve fit of tau during isovolumic relaxation.

Using the aforementioned methods, deformation can also be determined in the beating heart during the contraction phase or systole. During systole strain can be found in the myocardium. Strain is defined as the change in length divided by its original length. It is a dimensionless ratio of elongation with respect to a materials original length. Shear strain is the strain that acts parallel to the surface, or the amount of strain in one direction with respect to the other direction (Figure 2.4). Principal strain is the orientation plane of strain in which there is no shear strain. The maximal strain is the principal strain in the 1 direction and the minimal strain is the principal strain in the 2 direction which is orthogonal to the 1 direction. Plane strain

is used when the strain normal to the surface is assumed to be zero and can be oriented in any direction (Figure 2.4). To find the magnitude of plane strain in each direction and the shear strain (strain orthogonal to normal) Mohr's circle can be used as seen in Figure 2.5. Mohr's circle is the 2-D graphical representation of the state of strain at a point. Mohr's circle uses the following equations to construct it:

$$Center = \frac{1}{2}(\varepsilon_x + \varepsilon_y) \tag{5}$$

$$Radius = \sqrt{\left(\frac{1}{2}(\varepsilon_x + \varepsilon_y)\right)^2 + \left(\varepsilon_{xy}\right)^2} \tag{6}$$

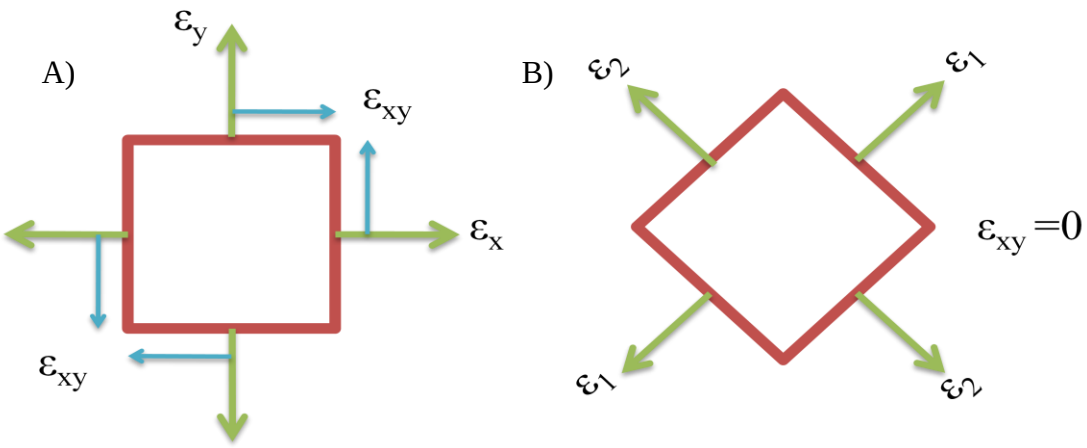

Figure 2.4: A) Graphical representation of strain (ε_x and ε_y) and shear strain (ε_{xy}). B) Graphical representation of principal strain (ε_1 and ε_2) (where shear strain is equal to zero)

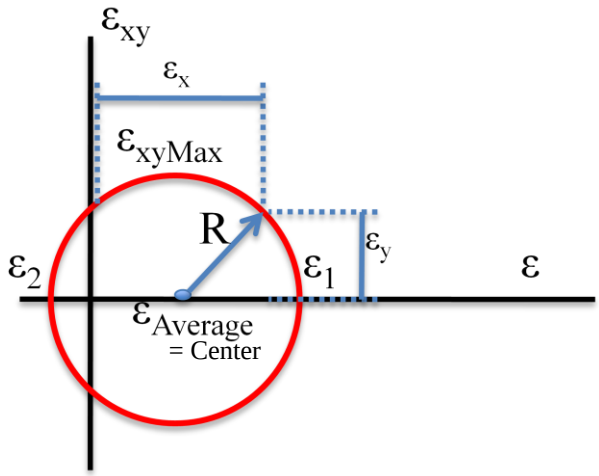

Figure 2.5: Mohr's Circle shows magnitude of plane strain based upon orientation. Used to find principal strains and maximal shear strain.

The strain in the 1 direction is the expansion of the myocardium during systole that is accounted for by the Poisson effect, which is a result of mass and volume conservation. Since the myocardium is incompressible, every contraction results in an expansion in a different direction in the wall. It has been shown that principal strain changes in both magnitude and angle before cardiac events[22-24]. Hankiewicz et al.[23] used MRI to measure principal strain changes in mice with heart failure. It was reported with heart failure the principal strain in the 1 direction decreased with advancement of heart failure compared to controls. In addition decreases in principal strains were detected prior to dilation of the ventricle[23]. Cupps and colleagues[24] used MRI to measure the principal strain orientation in the normal human left ventricle. The results yielded that principal strain in maximal contraction direction occurs in the circumferential-longitudinal plane that aligns with the apex to base axis of the heart[24]. This shows that orienting displacement data along the apex to base cardiac axis will provide the maximal contractile strain for the heart.

Another method of measuring displacements on the surface of the heart is sonomicrometry. Sonomicrometry uses piezoelectric crystals to send and receive an acoustic signal. The crystals must be sewn into the heart wall with acoustical conductivity between sending and receiving transducer crystals. The tissue should be homogeneous as only one measurement of distance is obtained between transducers thereby assuming displacement to be continuous. The change in time for the acoustic signal to travel between crystals determines the straight-line distance between the crystals. Sonomicrometry can be used to determine regional or global mechanics depending on the placement of the crystals. Regionally, sonomicrometry can be used to determine changes in distance in a specific area of the myocardium. This method can be used to determine regional strain in the myocardium.

While the methods described herein provide data for both systolic and diastolic function, there are several limitations to them as well. Both MRI and ECHO require expensive equipment to image the heart. Along with this equipment, MRI imaging can be time consuming. Further, to analyze the images from both MRI and ECHO requires a great deal of processing power. Finally, while MRI and ECHO are both non invasive, they are limited in spatial resolution because they are imaging through skin and bone and using the densities of the myocardium to determine location. To determine regional cardiac function with high spatial resolution over a large region of the heart an optical method was used that tracks the motions of random light intensity patterns. This optical method, HDM, uses high-resolution whole field images that allow the analysis of several locations within the region of interest. High-density

mapper is low cost and requires minimal processing power considerations, however the surface of the heart needs to be exposed to collect data.

2.4 High Density Mapper

High Density Mapper (HDM) tracks the motions of spatial patterns through a sub pixel extended phase correlation on the beating heart surface. HDM tracks random patterns instead of recognizable patterns such as particles, like most motion detection algorithms[25]. This improves the signal to noise ratio and increases the number of surfaces on which it is applicable[26]. Also, the distributions of grayscale values are transformed to the spectral domain to allow for faster data processing. The sub pixel accuracy of HDM makes it a useful tool to determine the contractile properties in the myocardium.

2.4.1 Image Processing

The mathematical basis of HDM has been documented previously[3, 27-30]. HDM is a technique for measuring the displacements on the surface of the heart. Briefly, HDM uses a Fourier based pattern tracking algorithm to determine the motion of a group of particles between consecutive images. First, the region of interest (ROI) is divided into a grid of smaller regions, each called a sub-image. In order to accurately access the whole field displacement, consecutive sub-images are overlapped 50% along both axes. For each sub-image, the unique light intensity distribution for both the deformed and undeformed states are used to determine the displacements x_0 and y_0 along the x and y axes, respectively. The light intensity distributions of sub-images are transformed from the spatial domain into the spectral domain using

discrete Fourier transforms (DFT). The following cross power spectrum correlates the independent spectra from the deformed and undeformed states:

$$\exp(-i(ux_0 + vy_0)) = \frac{\hat{f}_2(u,v)\hat{f}_1(u,v)^*}{\left|\hat{f}_2(u,v)\hat{f}_1(u,v)^*\right|} \qquad (7)$$

where $\hat{f}_1(u,v)$ is the 2-D DFT of the undeformed sub-image and $\hat{f}_2(u,v)$ is that of the deformed sub-image (* denotes a complex conjugate). In order to convert the phase change back to the spatial domain, an inverse Fourier transform is applied to the cross power spectrum, resulting in a dirac delta function with the peak located at the corresponding spatial shifts of the sub-image. In the spatial domain the impulse function obtained by the cross power spectrum is a downsampled Dirichlet kernel that is approximated as a sinc function. The sinc function is hyperbolically interpolated to determine the subpixel motion using:

$$C(x,y) \approx \frac{\sin(\pi(Mx - x_0))}{\pi(Mx - x_0)} \frac{\sin(\pi(Ny - y_0)}{\pi(My - y_0)} \qquad (8)$$

where the downsampling rates are M and N along the respective x and y axes. The procedure is then applied to each sub-image in a row-first order that results in a displacement matrix. Deformation within each sub-image is considered to be homogeneous. Thus HDM can be used to determine displacement of sub-images along two axes. Figure 2.6 shows a representative region of interest with sub-regions highlighted.

2.4.2 Post-processing of data

The HDM process results in a grid of vectors, each representing the displacement of a specific sub-image. The grid is broken down further where four points are used to determine area change using Green's theorem:

$$A = \frac{1}{2}\sum_{i=1}^{4}\left(x_i y_{i+1} - x_{i+1} y_i\right) \tag{9}$$

The displacement vectors are numerically differentiated to obtain strain tensors on the epicardial surface using Lagrangian strain equations:

$$E_{ij} = \frac{1}{2}\left[\frac{\partial u_i}{\partial X_j} + \frac{\partial u_j}{\partial X_i} + \frac{\partial u_k}{\partial X_i}\frac{\partial u_k}{\partial X_j}\right] \tag{10}$$

Where u and X represent the magnitude and direction of displacement, respectively, and E_{ij} represents the 2-D strain tensor. Because of the high image acquisition rate, Lagrangian strain magnitudes between frames are small; therefore the distinction between Lagrangian and Eulerian disappears reducing to Cauchy's infinitesimal strain tensor where higher orders of the derivatives were ignored:

$$e_{ij} = \frac{1}{2}\left[\frac{\partial u_j}{\partial x_i} + \frac{\partial u_i}{\partial x_j}\right] \tag{11}$$

In unabridged notation:

$$e_{xx} = \frac{\partial u}{\partial x} \tag{12}$$

$$e_{yy} = \frac{\partial v}{\partial y} \tag{13}$$

$$e_{xy} = \frac{1}{2}\left[\frac{\partial u}{\partial y} + \frac{\partial v}{\partial x}\right] \tag{14}$$

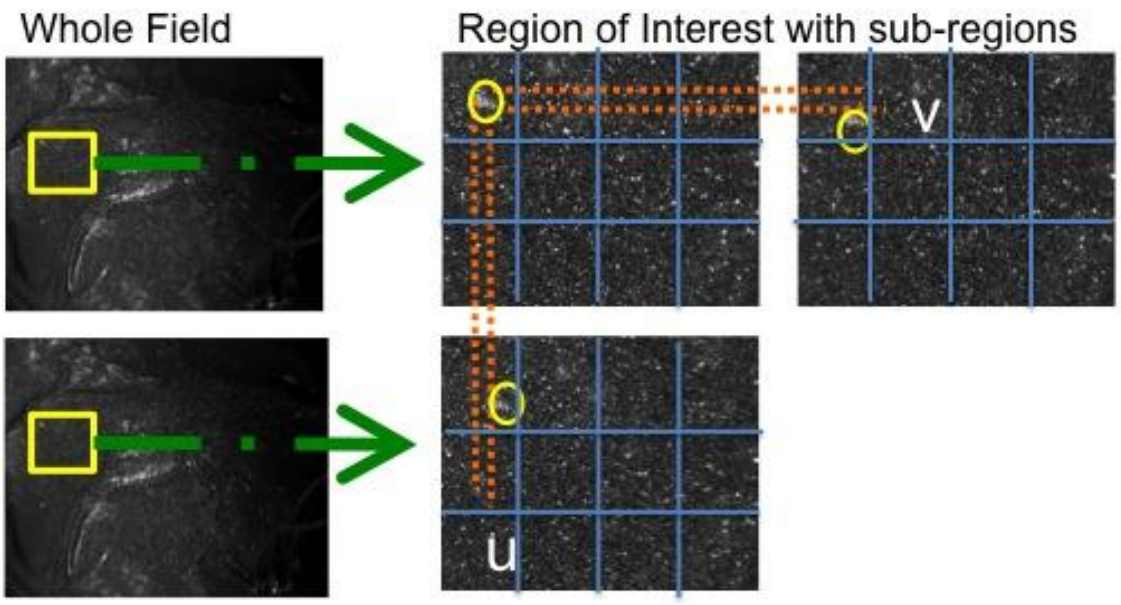

Figure 2.6: Example of region of interest in HDM using two consecutive frames to determine displacement with sub-regions highlighted in blue (u is change in x direction)(v is change in y direction)

2.5 Pacing

Arrhythmias occur when the heart does not conduct properly. They last from seconds to minutes and are potentially life threatening. To correct certain types of arrhythmias a pacemaker, consisting of a battery, microcontroller housing, and leads, can be inserted into either the atria or the ventricle. Worldwide there are about 3,000,000 people with pacemakers and each year approximately 600,000 are implanted[31]. Most pacemakers are used as a device therapy to treat bradycardia. When the heart's natural pacemaker cells are damaged, but conduction to the ventricles remains intact, in conditions such as sick sinus syndrome, the leads are inserted in the atria. Conversely when the normal conduction pathway that allows the flow of ions from the atrium to the ventricle is inhibited, due to AV node block or

bundle branch blocks, the leads are implanted in the ventricle. Attaching the leads to the ventricle allows the ventricle to contract at a rate set by the pacemaker, although the atria will likely not contract in sync with the ventricles.

Ventricular pacing was thought to be a non-damaging intervention to cellular and sub cellular function[31]. It is now known that this is not the case as ventricular pacing causes regional changes to both the cellular response and the mechanical response in the region closest to the electrode. Several studies have shown the effects of ventricular pacing on the mechanics of the ventricle[2, 3, 9, 32, 33]. The regional activation time and maximum change in pressure of the ventricle relates linearly to the regional fiber strain generally in the direction of the principal strain as studied by Delhaas et al[2]. Optical markers were used in 16 regions and images recorded on video to measure displacements, while an electrode brush measured activation time. Electrical asynchrony, or changing of normal activation times, of more than 30 ms causes non-uniformities in regional fiber strain[2]. Prinzen et al.[9] used MRI tagging on canine models and found ventricular pacing systolic fiber strain and work are approximately zero in the regions nearest the pacing site and they increased at a distance from the pacing site. The study concluded that ventricular pacing causes a three-fold difference in myofiber work within the left ventricular free wall. Azeloglu et al.[3] used an optical method, similar to HDM, to track surface displacement and discovered that changing the location of the electrode changes the regional stroke work and systolic area contraction in the region nearest the pacing electrode. By keeping the same region of interest and shifting electrode location they showed that the mechanical function in the region of interest changes with the shift in electrode

location[3]. Thus, ventricular pacing changes the contraction of the left ventricle by changing activation times, decreasing strain, and decreasing work.

Torsion of the ventricle plays a vital role in the proper filling and ejection mechanics. The rotation permits the endocardium to contract more than the epicardium. Torsion changes during ventricular pacing especially in the left ventricle[34]. Sorger et al.[34] used MRI tagging on canine models to evaluate the effects of pacing on the left ventricle. They concluded that pacing the ventricle decreases the efficiency of diastole, resulting in an overshoot of baseline values at end diastole.

In summary, ventricular pacing changes the mechanics of the ventricle and the stretch of the myocardium, these changes are likely associated with molecular or physiological changes.

2.6 Cardiac Memory

Cardiac memory was originally defined by T-wave changes that occur after electronic pacing. Chatterjee et al.[4] reported on 31 patients in an un-paced state after ventricular pacing. This observational study concluded that 29 of the 31 patients showed T-wave inversion and S-T depression in both the limb and pre-cordial leads. The study found there is no myocardial damage from the electrode and the rate of dissipation is directly related to the duration of artificial pacing. The study concludes there was no clinical evidence of deterioration of function in the myocardium and the changes are a manifestation of a reversible abnormality[9].

In 1982, Rosenbaum et al. studied the changes in T-wave formation due to left bundle branch block (LBBB) and right ventricular pacing. LBBB causes

instantaneous inversion of the T-wave opposite to that of the main QRS forces, this being considered a secondary T-wave inversion. Right ventricular pacing also caused a T-wave change, however it was not instantaneous as seen in LBBB. The first changes were a notching or flattening of the T-wave that eventually manifested into negative T-waves after 10 minutes. The changes gradually progressed uniformly for the first 30 to 60 hours of pacing with a maximal effect shown after 12-14 days of pacing and the return to normal took an equal time period. The authors found that faster pacing times induce shorter T-wave change times and that the effects will accumulate over time. They conclude by suggesting that the heart memory effect is not the same as the processes in storage and retrieval of data but instead an electrophysiological response.

Cardiac memory is measured using vectorcardiography, a graphic display of the electrical activity of the heart from the summation of three vectors. The electrical forces from the heart are recorded as vectors with length representing magnitude and direction in relation to the body and polarity as positive and negative[35]. Changes in the magnitude and direction of T-wave vector are representative of cardiac memory[6]. Cardiac memory can also be seen on an electrocardiogram as a flattening or inversion of the T-wave that represents the repolarization of the ventricle independent of the atria (Figure 2.7).

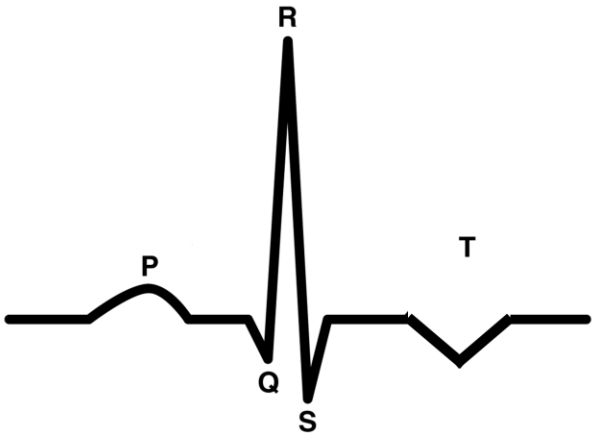

Figure 2.7: Electrocardiogram with inverted T-Wave

2.6.1 Short-term Cardiac Memory

Short-term cardiac memory is induced after a period of altered activation for 15 minutes to two hours with memory lasting minutes to hours after return to normal activation[4, 5, 36]. This time period was chosen based upon the work of Rosenbaum et al.[5] and previous studies have shown this time period to be appropriate to induce short-term cardiac memory[37-40].

Studying the electrophysiology of short-term cardiac memory has given some insight into the underlying mechanisms. Janse et al.[39] found under control conditions of atrial pacing, a left ventricular apicobasal gradient is seen with the shortest repolarization times anterobasally and the longest posteroapically. There was no significant transmural repolarization gradient in control groups or after induction of cardiac memory. Inducing short-term cardiac memory shortened both repolarization time and monophasic action potential durations. Suggesting that the deeper T-wave

in the ECG might be explained by a more rapid phase 3 repolarization of the action potential[39].

Ventricular pacing alters ventricular activation that initiates memory by altered ventricular stretch and contractile patterns[41]. Sosunov et al.[41] measured the T-wave vector displacement from vectorcardiography to determine if cardiac memory was induced from ventricular pacing, using isolated rabbit hearts that were stimulated from both the atria and ventricle to contract isovolumically. The hearts volume did not change during contraction so it was considered stretched. Finally concluding that since the hearts were not under any loading conditions besides stretch that altered stretch induces cardiac memory and also altered coronary flow, ischemia or structural remodeling is not associated with cardiac memory[42]. Altered angiotensin II, in response to increased stretch, also seems to have an effect on short-term cardiac memory[43]. Ricard et al.[43] determined that altering myocardial stretch through ventricular pacing activates angiotensin II synthesis in myocytes by using canine models to determine the effects of angiotensin II on cardiac memory by measuring the T-wave through vectorcardiography and injecting angiotensin II receptor blockers.

2.6.2 Long-term Cardiac Memory

Long-term cardiac memory is induced after a period of two to three weeks of altered activation resulting in memory lasting weeks to months[8, 36, 37, 43]. The magnitude of T-wave change increases over time and persists for longer intervals. The initiation of long-term cardiac memory was studied on isolated tissue slabs of

canine hearts paced from the left ventricle by Shvilkin et al.[8] Transmyocardial repolarization gradient changes were observed because of increased action potential durations in the left ventricular endocardium and epicardium, but not midmyocardium. Others have mapped the repolarization gradients during altered activation and have observed changes in the gradient from a normal activation repolarization gradient to decreased repolarization gradients[42, 44].

Along with changes in the repolarization gradient, groups have studied changes in ion channels due to outward currents, inward currents, connexins, transcription, and transduction. I_{to} shows a transmural gradient in the ventricle. Epicardial I_{to} has a more negative voltage threshold for activation, a more negative midpoint of inactivation, is larger in amplitude, and has a faster recovery from inactivation than endocardium[45]. In long-term cardiac memory the epicardial action potential has a longer duration and a loss of the "notch" that is determined by I_{to}. The channel subunit contributing to I_{to} is the pore-forming unit in humans and canine models Kv4.3, with accessory protein KChIP2, important because the accessory protein KChIP2 is not only for Kv4.3 but also for the inward current $I_{Ca(L)}$[40].

Microelectrode recordings used in an isolated tissue model showed a loss in the outward potassium current I_{to} that determines the action potential notch. Yu et al.[46] showed that cardiac memory alters the kinetics and decreases the density of the outward potassium current I_{to1} by inducing long-term cardiac memory then removing the tissue and performing whole cell patch clamping[46]. However, there is a prolonged and elevated action potential duration that cannot be explained by I_{to1} alone.

Connexins that make up gap junctions are remodeled by left ventricular pacing to change myocardial activation[47]. Gap junctions are a specialized intercellular connection between cells. Gap junctions allow for molecules and ions to pass freely between cells and are essential to contraction in the heart because they allow for ions to pass between myocytes inducing them to contract simultaneously. A reduction in connexin43 density, the most abundant gap junction protein found in the ventricle, along with remodeling in a gradient away from the pacing site, is seen with left ventricular pacing[47].

Fiber strain and workload over the left ventricular freewall are altered during ventricular pacing[9], which relates to the angiotensin II synthesis by altered stretch. Shyu et al.[48] cyclically stretched neonatal rat cardiac myocytes, using a flexcell device (a device that uses a vacuum to stretch silicone membranes), and measured the amount of angiotensin II released and found that increased stretch increases angiotensin II and connexin43 expression. Dodge et al.[49] cultured neonatal rat cardiac myocytes and increased amounts of angiontensin II to show an increase in the amount of connexin43 expressed. Given these results it is possible that angiotensin II has a role in the remodeling of connexin43 in cardiac memory.

Influenced by cAMP response element binding protein (CREB) contribution to central nervous system memory, Patberg et al.[7] studied the levels of CREB in the heart after ventricular pacing. They found decreased levels of CREB in the left ventricle after inducing short-term cardiac memory and long-term cardiac memory. Decreased CREB is angiotensin-modulated and calcium dependent in short-term

cardiac memory and in long-term cardiac memory the activity in the Kv4.3 promoter can explain the I_{to} down regulation[7].

In summary, altering stretch changes the expression of different proteins that lead to inducing cardiac memory. Stretch can be altered by many different protocols including ventricular pacing.

3 Hypothesis and Specific Aims

3.1 Hypothesis

Ventricular pacing changes the activation patterns of the heart. This change leads to changes in mechanical function near the pacing site. After pacing cession T-wave, electrophysiological changes remain that are consistent with ventricular pacing. There are also electrical activation gradients and mechanical gradients seen during ventricular pacing. Further, there is a protein gradient seen after 2 hrs of ventricular pacing upon return to normal activation pathways. **Therefore we hypothesize that the mechanical function in the region around the pacing site will continue to be altered after cession of pacing, in effect showing a mechanical cardiac memory.** Computing regional stroke work and systolic area contraction around the pacing site will test this hypothesis.

3.2 Specific Aim 1

Determine if there is a regional mechanical correlation to short-term cardiac memory.

We will evaluate the regional function (regional stroke work and systolic area contraction) of the heart in the area closest to the pacing electrode, before, during, and after ventricular pacing. These data will be compared to animals that are atrially paced for two hours. Also, we will evaluate global function (maximum and minimum change in pressure vs. time, diastolic relaxation constant, and developed pressure) before, during, and after ventricular pacing and compare it to atrially paced animals.

3.3 Specific Aim 2

Determine if systolic or diastolic function is altered after cessation of short term ventricular pacing.

We will evaluate regional principal strains during systole and diastolic twist over the entire region of interest and in sub-regions of interest. These will again be evaluated before, during, and after ventricular pacing and the time points will be compared.

4 Materials and Methods

4.1 Animal Surgery

All animals received humane care in compliance with the "Principles of Laboratory Animal Care" formulated by the National Society for Medical Research and the "Guide for the Care and Use of Laboratory Animals" prepared by the National Academy of Sciences and published by the National Institutes of Health (NIH Publication No. 85-23, revised 1985). The IACUC of the Columbia University approved the protocol. For acute studies, mongrel dogs 1-3 years old, weighing 22-26 kg, were anesthetized with thiopental 10-17 mg/kg IV or propafol 10 mg/kg, intubated, and ventilated with isoflurane (1.0-4.0%) and oxygen (two L /min). A left thoracotomy was performed to expose the heart. The left femoral artery was catheterized to monitor blood pressure and the heart was suspended in a pericardial cradle.

4.2 Pacing

Bipolar pacing electrodes were attached to the atrium and left ventricle as show in Figure 4.1. All animals were subjected to a 40-minute atrial pacing stabilization period to create a baseline for continuity across experiments. All animals were paced at 150 beats per minute (bpm). After the stabilization period, atrial pacing was continued in four animals. Data was collected starting at the end of the stabilization period (time equals zero) and every half hour for two hours (control). The remaining six animals were paced from the ventricle while data was collected every 30 minutes

(memory). At the one and two hour time points pacing was switched over to the atrium to collect data and immediately switched back to the ventricle after data collection (Figure 4.2). A 6 lead ECG was continuously recorded.

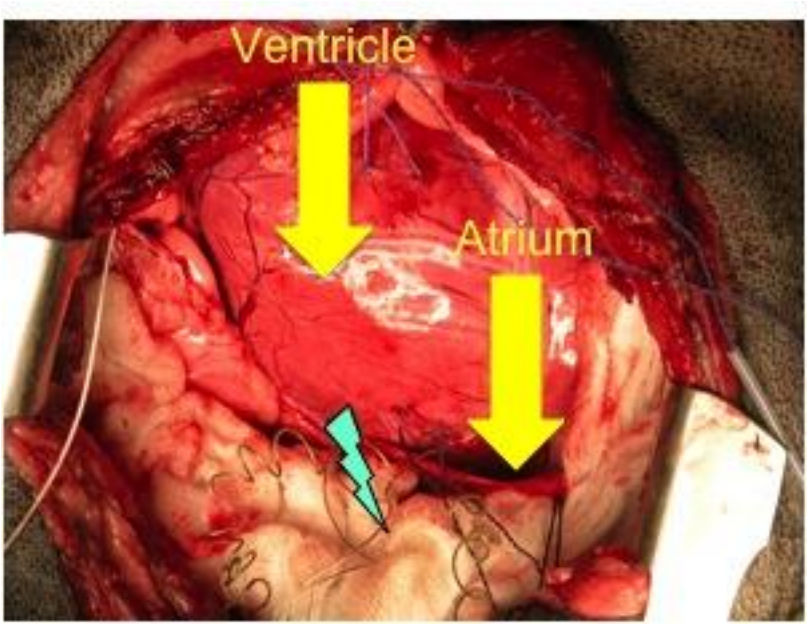

Figure 4.1: Pacing electrode placement in the atrium and ventricle.

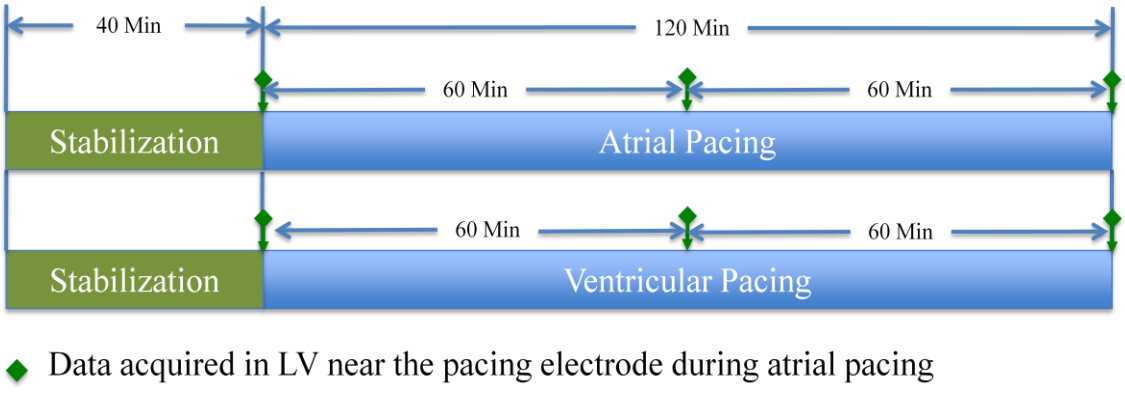

Figure 4.2: Pacing protocol timeline

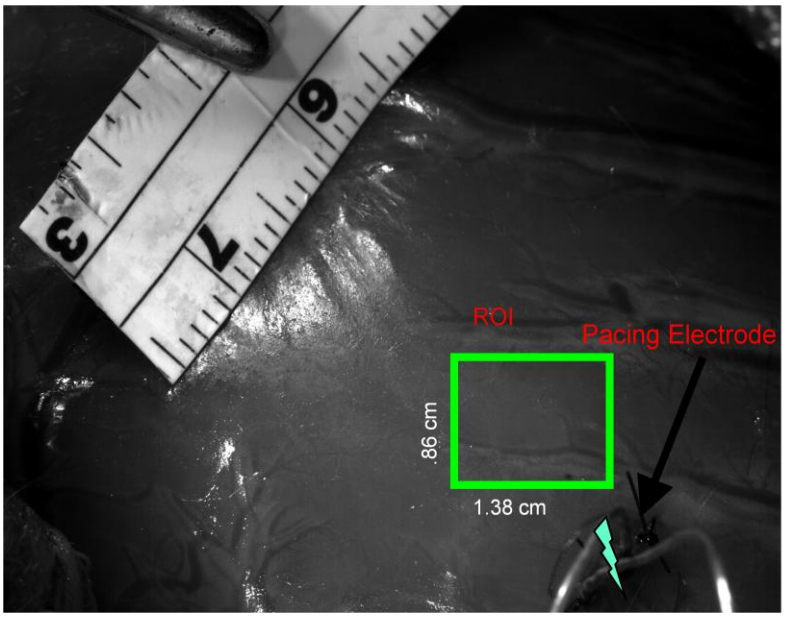

Figure 4.3: Determination of scale by pixels per centimeter

4.3 Data Acquisition

A pressure transducer (Millar instruments; Houston, TX; Model # SPR-524) was inserted into the left ventricle (LV) through the apex of the heart. After the 45-minute stabilization period, a mixture of silicon carbide particles (40μm diameter) and retro-reflective beads (60μm diameter) was applied to create a random light distribution in the region of interest. After focusing on the region of interest on the anterior of the heart, images were acquired at 125 frames per second using a complimentary metal-oxide semiconductor (CMOS) camera (Photron; San Diego CA; Model # Fastcam-X 1280 PCI) with a resolution of 1280 x 1024 pixels and 8 bit pixel depth. The left ventricular pressure was simultaneously obtained using an analog-digital converter (National Instruments; Austin, TX; Model # PCI-6023E) and the camera connected to

a one-gigabyte frame grabber board (Photron; San Diego, CA). Data were collected simultaneously for 8 seconds at 125 Hz. All data was saved on a Windows based PC.

4.4 Global Function

Four measures of global function were determined. Isovolumic relaxation time constant, developed pressure, maximum change in pressure, and minimum change in pressure. Tau is the relaxation time constant of the heart and is determined by Equation 15. The duration of isovolumic relaxation during which Tau is calculated using Equation 15 (Figure 4.4).

$$P = P_0 + e^{\frac{-t}{\tau}}$$
$$\tau = -\frac{t}{\ln|P|} \qquad (15)$$

Developed pressure is the maximum pressure developed in the left ventricle as measured by the inserted pressure transducer minus the minimum pressure. Maximum and minimum change in pressure is the slope of the pressure vs. time plot between consecutive frames.

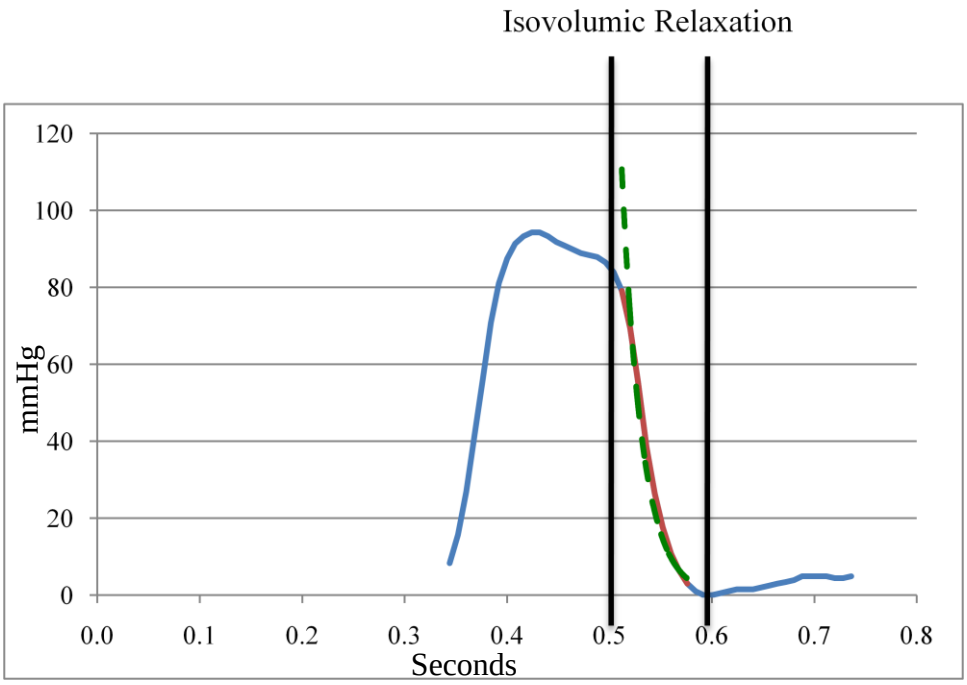

Figure 4.4: Tau is the exponential fit to the pressure (mmHg) versus time (s) during isovolumic relaxation

4.5 Specific Aim 1: Mechanical Analysis

Discrete integration of the pressure versus area (Figure 4.5), from end diastole to end diastole (from frame to frame), was used to determine regional stroke work according to Green's theorem[28]:

$$RSW = \int P \cdot dA \qquad (16)$$

Systolic area contraction, another measure of mechanical contractility was also determined. Systolic area contraction was determined by the change in area of the region of interest from end diastole to end systole (Figure 4.6). It is computed by subtracting the normalized area at end systole from the normalized area at end diastole[28].

$$SAC = \frac{A_{end-diastole} - A_{end-systole}}{A_{end-diastole}} \quad (17)$$

In order to evaluate mechanical cardiac memory, regional stroke work and systolic area contraction were measured during atrial pacing at the initial time point (Figure 4.2). Those results were compared to regional stroke work and systolic area contraction during atrial pacing after two hours of ventricular pacing (Figure 4.2). Also with each time point, the region of interest was broken down into nine different sub-regions (Figure 4.7). Regional stroke work and systolic area contraction were determined in the each of the sub-regions and comparisons were made between the site closest to the pacing electrode and the site furthest from the pacing electrode.

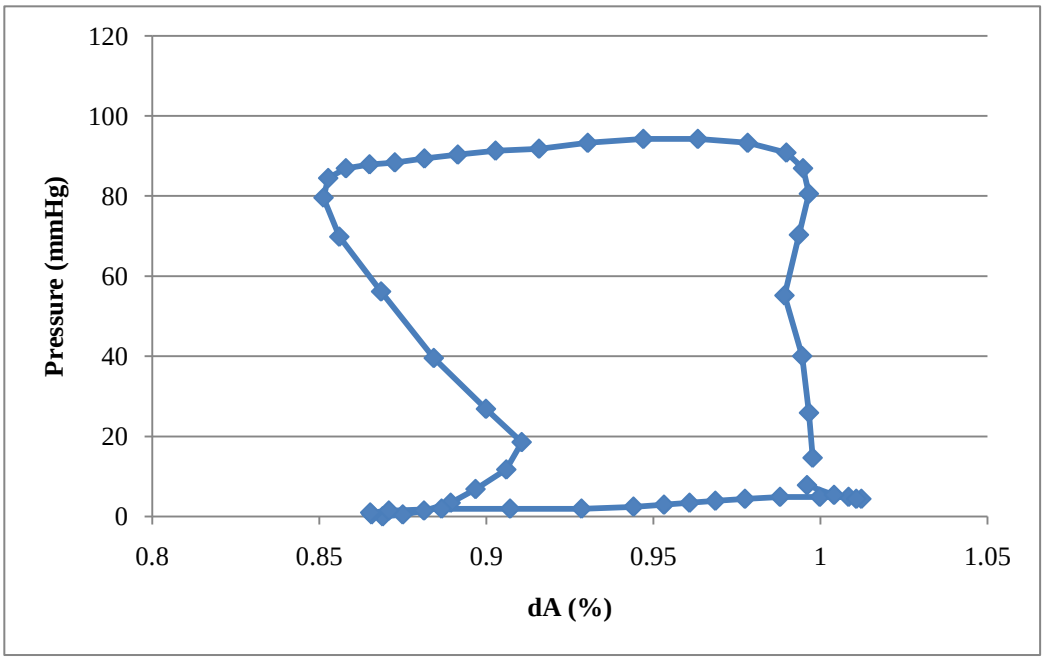

Figure 4.5: Discrete integration of work loop leads to regional stroke work

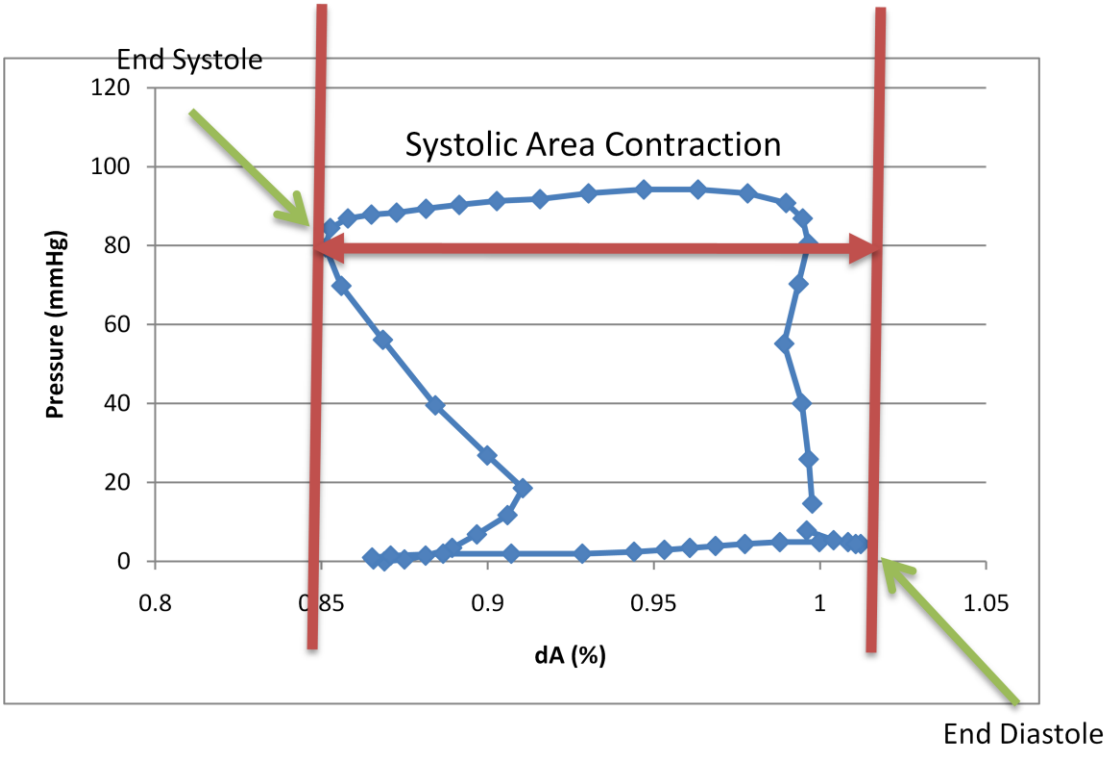

Figure 4.6: Determination of systolic area contraction by subtracting the area at end systole from the area at end diastole.

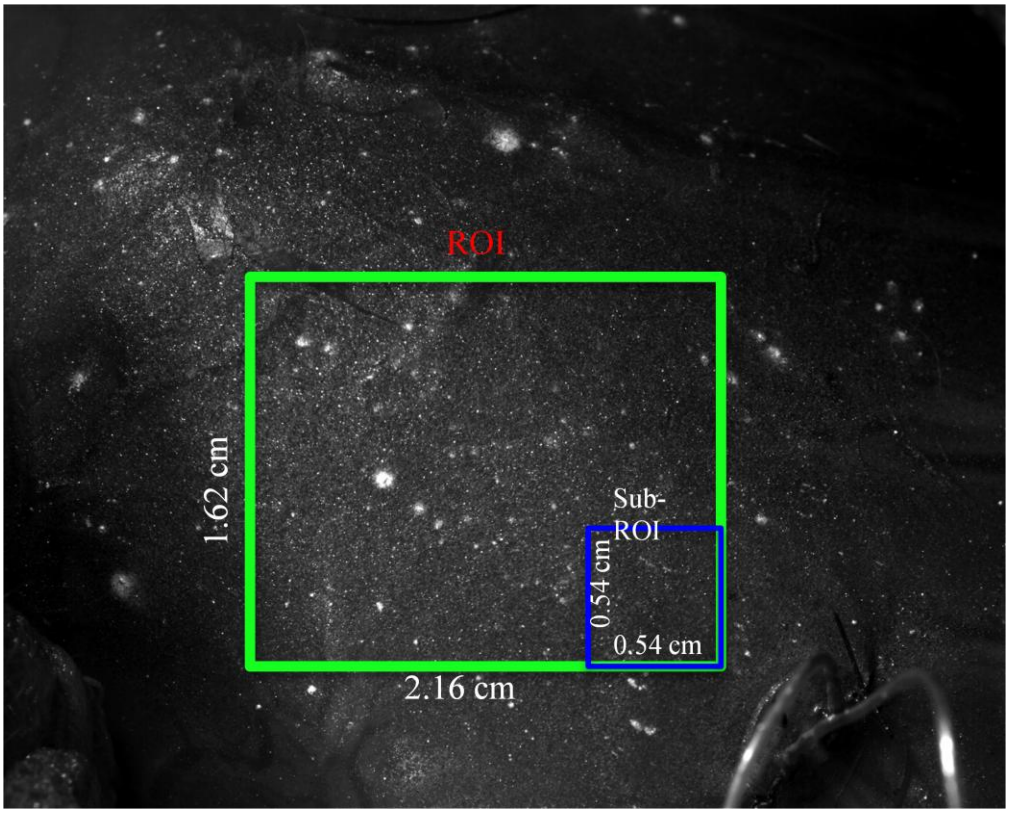

Figure 4.7: Region of interest with a single sub-region highlighted. The region was broken into 9 separate sub-regions.

4.6 Specific Aim 2: Diastolic Twist

The magnitude and rate of diastolic shear on the epicardial surface can be used as a measure of regional diastolic function[50]. Vector displacement maps from HDM were used to calculate epicardial shear through infinitesimal Eulerian strain equations, the vector displacement matrices were converted from the camera coordinate system to the heart coordinate system by measuring the angle between the x-axis and the left anterior descending artery (LAD) via image correlation software. Each vector from the displacement matrices was rotated using Equation 17 to acquire rotated vector displacement matrices x' and y'.

$$x' = u\cos\theta + v\sin\theta$$
$$y' = u\sin\theta + v\cos\theta \quad (18)$$

These were then converted to Lagrangian strain using Equation 10. The shape of the heart is assumed cylindrical so that shear due to torsion (γ) is assumed linear along the ventricular radius and defined as the gradient of surface rotation with respect to the cardiac axis, that can be show as follows:

$$du = r \cdot \sin d\phi \quad (19a)$$

$$\tan d\phi \approx d\phi \quad (19b)$$

$$du = r \cdot d\phi \quad (19c)$$

$$\gamma = \frac{r d\phi}{dz} = \frac{du}{dy'} \quad (19d)$$

$$\dot{\gamma} = \frac{\partial}{\partial t}\left(\frac{du}{dy'}\right) \quad (19e)$$

Figure 4.8 is a graphic representation of the determination of diastolic twist.

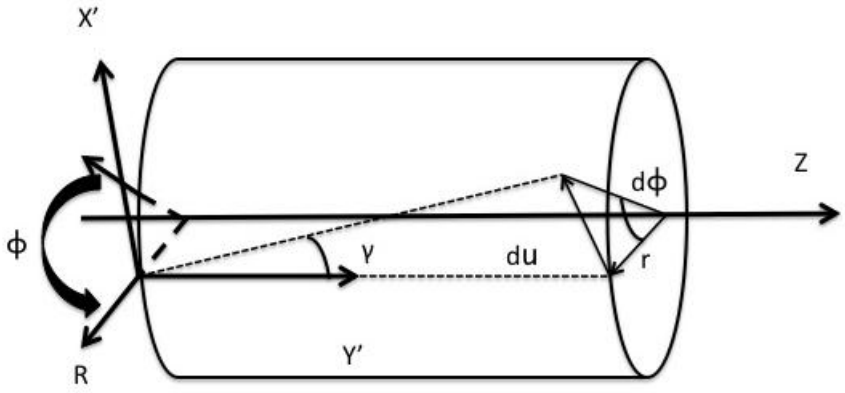

Figure 4.8: 2-D coordinate system of the camera is denoted with X'Y' where the cylindrical cardiac axes are denoted with ZRϕ

4.7 Specific Aim 2: Systolic Principal Strain

The principal strain was determined by adjusting the strain vectors to the plane in which there is no shear strain, thus giving two principals strains (Equation 20). Systolic principal strain was determined by the summation of strain vectors from the start of systole to the end of systole (Equation 21) and calculating the principal strain by Equation 20. Equation 22 determined the angular orientation of the principal plane.

$$\varepsilon_{1,2} = \frac{\varepsilon_x + \varepsilon_y}{2} \pm \sqrt{\left(\frac{\varepsilon_x - \varepsilon_y}{2}\right)^2 + \left(\frac{\varepsilon_{xy}}{2}\right)^2} \tag{20}$$

$$\varepsilon_{x,y} = \sum_{Systole} \varepsilon_{x,y}$$
$$\varepsilon_{xy} = \sum_{Systole} \varepsilon_{xy} \tag{21}$$

$$\tan 2\theta_p = \frac{2\varepsilon_{xy}}{\varepsilon_x - \varepsilon_y}$$
$$\theta_p = \frac{1}{2}\tan^{-1}\left(\frac{2\varepsilon_{xy}}{\varepsilon_x - \varepsilon_y}\right) \quad (22)$$

The principal strains were found in two directions, the maximal being the 1 direction and the minimal being the 2 direction. Along with the magnitudes, the angle for the 1 direction was found, with the angle for the 2 direction being 90° from the 1 direction. The principal strain is the orientation in which there is no shear strain. Figure 4.9 shows principal strains in the 1 and 2 directions acting along the heart that was determined by the LAD. Maximal contraction occurs in the 2 direction which is aligned with the fibers. The cardiac axis is considered to be from base to apex.

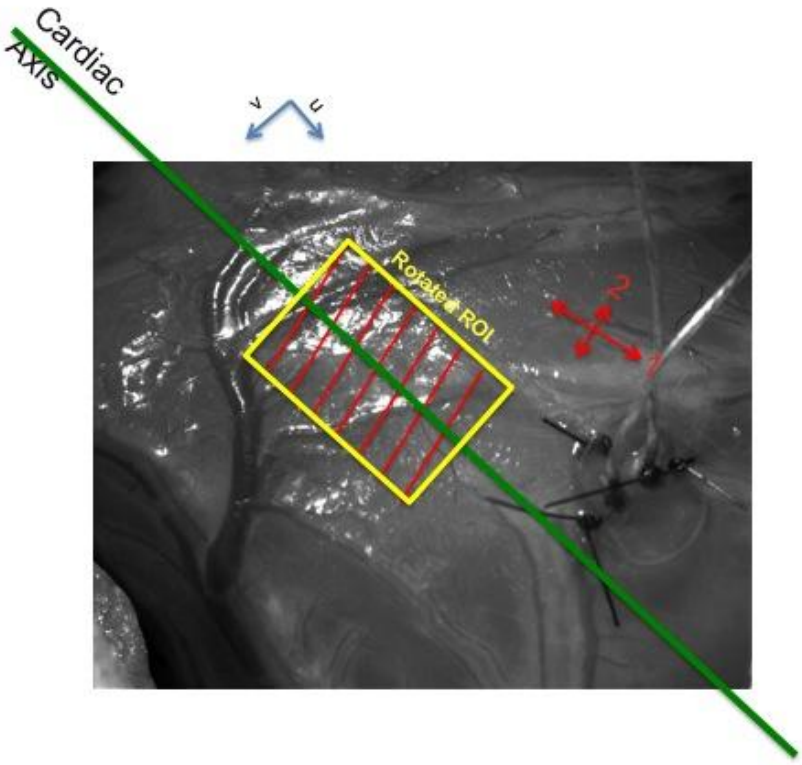

Figure 4.9: Graphical depiction of principal strains and orientation to the cardiac axis that was determined by the lateral anterior descending artery.

4.8 Statistics

A two-way unpaired student's T-test was performed to test for the statistical significance between cardiac memory and control groups. Two-way paired students T-test was performed to test for the statistical significance between time point measurements within the cardiac memory and control groups. The null hypothesis was rejected when $\alpha \leq 0.05$. All data are represented as mean ± standard error of the mean (SEM). For the global function parameters, a one-way ANOVA with post hoc tukey comparison was used to determine statistical significance across groups.

ANOVA was used for the global function to compare the five time points at the same time.

5 *Results*

5.1 Global Function

Tau was calculated for 9 animals (4 control, 5 cardiac memory). The results showed no statistical differences between the two groups (control vs. cardiac memory) or between time points within each of the groups. No statistical difference was found in developed pressure between groups or between time points within the groups. Finally dP/dt_{max} and dP/dt_{min} were calculated for the same nine animals with no statistical difference between the two groups or between time points within the groups (Table 5-1).

Table 5-1: Global function results show no difference in any parameter measured between baseline and two hours of pacing. Data: mean ± SEM

	Control (n=4)		Cardiac Memory (n=5)		
	Baseline	2 Hours AP	Baseline	Ventricular Pacing	2 Hours
Tau (ms)	51.3 ± 3.7	64.6 ± 7.2	49.1 ± 6.7	57.7 ± 7.3	59.0 ± 7.0
Developed Pressure (mmHg)	86 ± 4	98 ± 4	80 ± 4	74 ± 3	81 ± 3
dP/dt_{max} (mmHg/s)	3142 ± 261	3150 ± 350	2904 ± 216	2222 ± 170	3204 ± 418
dP/dt_{min} (mmHg/s)	-2616 ± 305	-2411 ± 214	-2343 ± 185	-2149 ± 187	-2930 ± 254

5.2 Specific Aim 1: Mechanical Correlation to Cardiac Memory

To determine if a mechanical correlation to cardiac memory exists, regional stroke work and systolic area contraction were measured in nine animals (four control, five cardiac memory). Regional stroke work determines the functional output from the region of interest while the systolic area contraction determines the contraction of the region of interest during one full cardiac cycle.

The average region of interest size was 120.6 ± 35.2 mm^2. The deformation of the heart surface was imaged with a resolution of 36.5 ± 3.9 μm/pixel. The baseline regional stroke work was not different between the two groups (control 4.9 ± 3.2%; cardiac memory 6.0 ± 3.3%; $p>0.05$). Further, systolic area contraction at baseline was not different between the two groups (control 9.8 ± 6.5%; cardiac memory 5.0 ± 6.6%; $p>0.05$).

After two hours of atrial pacing, regional stroke work in the control group was not statistically different than the baseline measurement in the control group (control 5.7 ± 2.6%). Whereas, after two hours of ventricular pacing, upon return to normal electrical activation pathways (atrial pacing), the regional stroke work in the cardiac memory group was statistically higher than during ventricular pacing and lower than baseline measurement (cardiac memory 2.4 ± 1.6%; VP -3.8 ± 0.9%; $p<0.05$ (paired t-test)). Figure 5.1 shows regional stroke work results for all groups. Figure 5.2 shows representative work loops from control and cardiac memory groups at both the initial time point and after two hours of ventricular pacing.

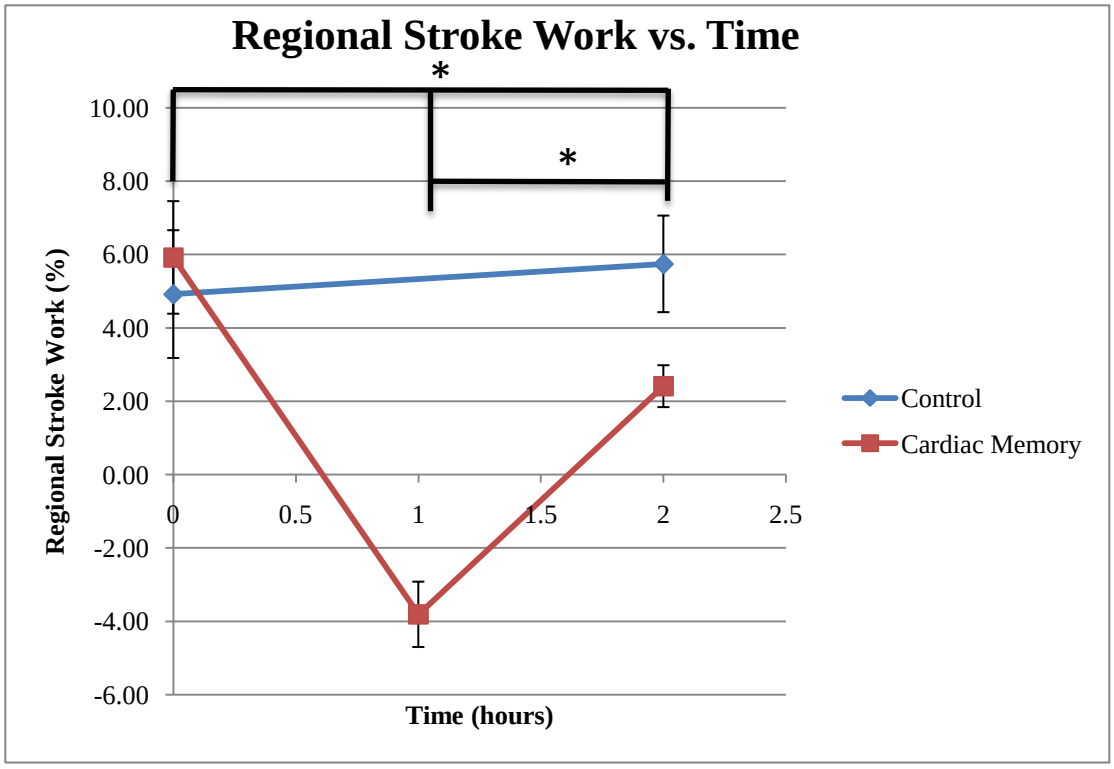

Figure 5.1: Regional stroke work vs. time. Significant differences in all time points from the cardiac memory group were noted (* denotes $p<0.05$ vs t=0). The results suggest ventricular pacing decreases the regional stroke work and after 2 hours of ventricular pacing upon return to normal electrical activation pathways the decrease remains compared to control values

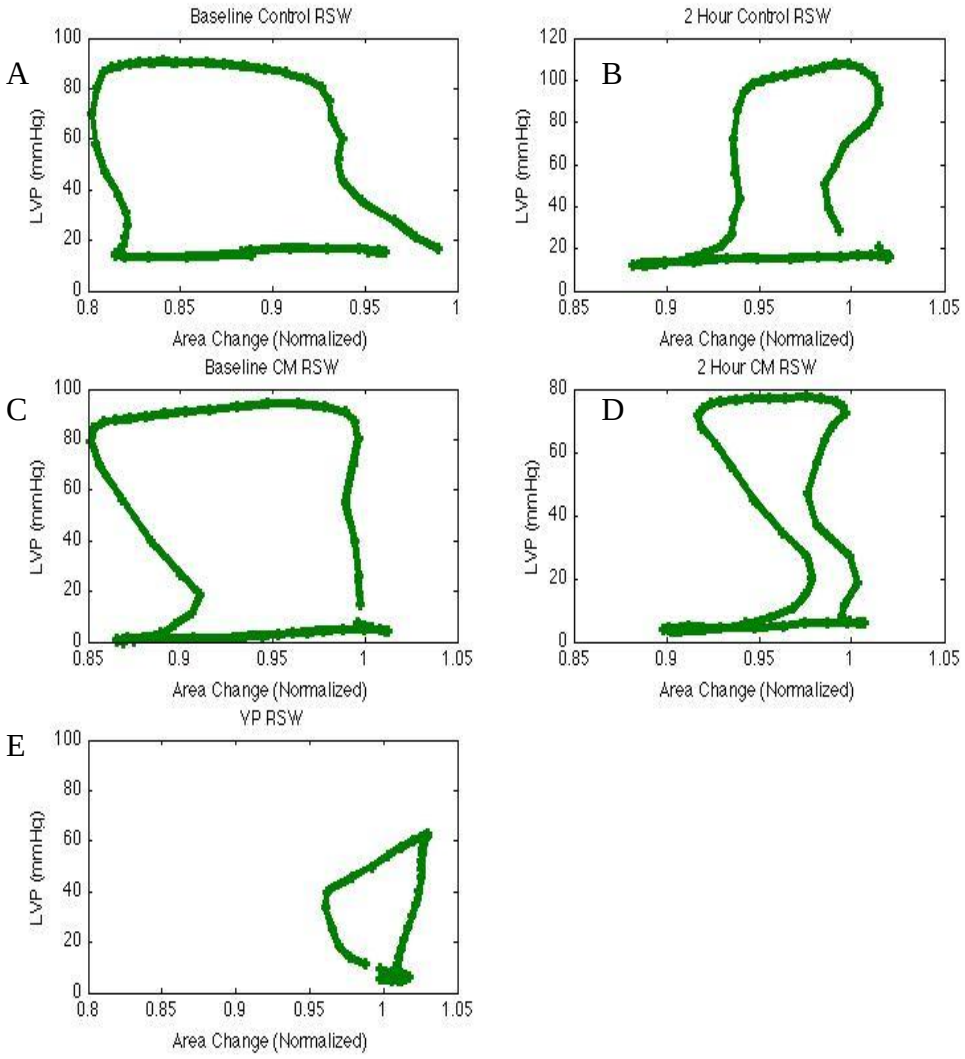

Figure 5.2: A) Workloop from a control animal at t=0 B) Workloop from a control animal after 2 hours of AP C) Workloop from a cardiac memory animal at t=0 D) Workloop from a cardiac memory animal after 2 hours of ventricular pacing upon return to normal activation pathways (atrial pacing) E) Workloop from a cardiac memory animal during ventricular pacing (t=1hour). All workloops are in the counter-clockwise direction.

Systolic area contraction in the control group after two hours of atrial pacing was not significantly different than baseline (control 9.3 ± 2.6%). However, after 2 hours of ventricular pacing, upon return to normal activation pathways (atrial pacing),

systolic area contraction in the cardiac memory group was significantly lower than baseline for the cardiac memory group (cardiac memory 0.2 ± 7.4%; $p<0.05$). Further, systolic area contraction during ventricular pacing (-6.2 ± 2.0%) was significantly lower than baseline for the cardiac memory group ($p<0.05$), whereas systolic area contraction after 2 hours of ventricular pacing, upon return to normal activation pathways (atrial pacing), was not significantly different than during ventricular pacing. Figure 5.3 shows systolic area contraction results from all groups.

As function changes with respect to distance from the pacing electrode, a larger region of interest was analyzed to determine the difference in function with proximity to the pacing electrode. The control group was not exposed to ventricular pacing, therefore only memory canine models were analyzed with a larger region of interest. The average larger region of interest was 444.9 ± 105.2 mm^2 with an image acquisition resolution of 36.5 ± 3.9 μm/pixel and sub-region of interest size 37.1 ± 2.9 mm^2. At baseline regional stroke work close to the electrode (2.3 ± 1.4%) was not significantly different than the region furthest from the electrode (3.9 ± 1.1%). After two hours of ventricular pacing, upon return to normal activation pathways (atrial pacing), there was a significant difference in regional stroke work between the area closest to the pacing electrode (-1.5 ± 0.5%) and the region furthest from the pacing electrode (2.1 ±1.1%; $p<0.05$). Finally, the region nearest the pacing electrode was lower than baseline after two hours of ventricular pacing upon return to normal activation pathways (atrial pacing)($p<0.05$). Figure 5.4 is a bar graph showing the results from the sub-ROI break down. Also Figure 5.5 shows representative images of the regional stroke work gradient across the entire ROI. To determine if there was

a linear relationship between distance from the pacing electrode and regional stroke work, as suggested by Azeloglu et al[3], regional stroke work was plotted as a function of distance. The results herein yielded low correlation to a linear fit and therefore suggest it is not a linear relationship (Figure 5.6).

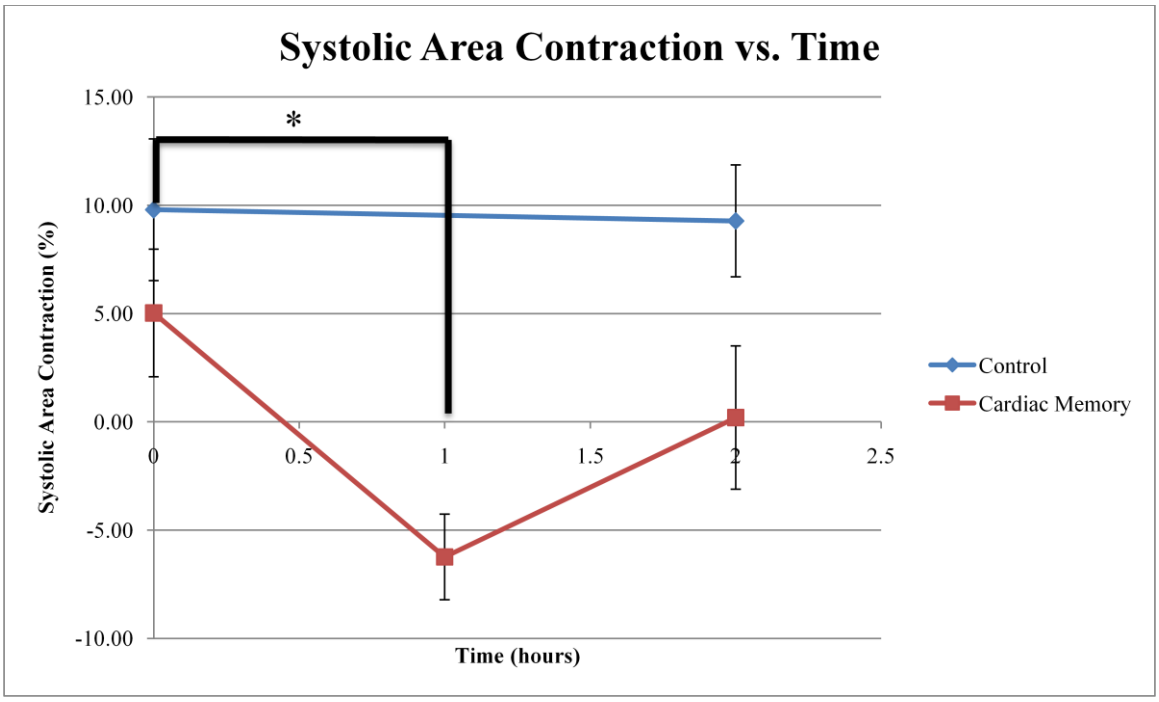

Figure 5.3: Systolic area contraction vs. time. Significant difference between baseline and ventricular pacing were seen in cardiac memory group (* denotes p<0.05). The results suggest that ventricular pacing decreases systolic area contraction.

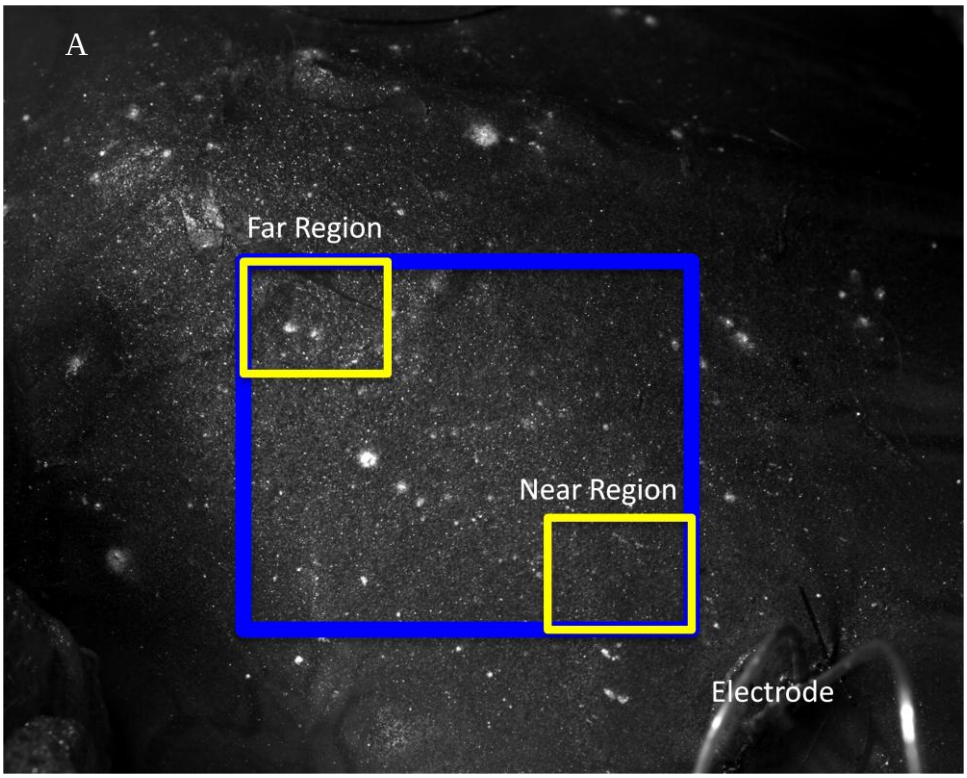

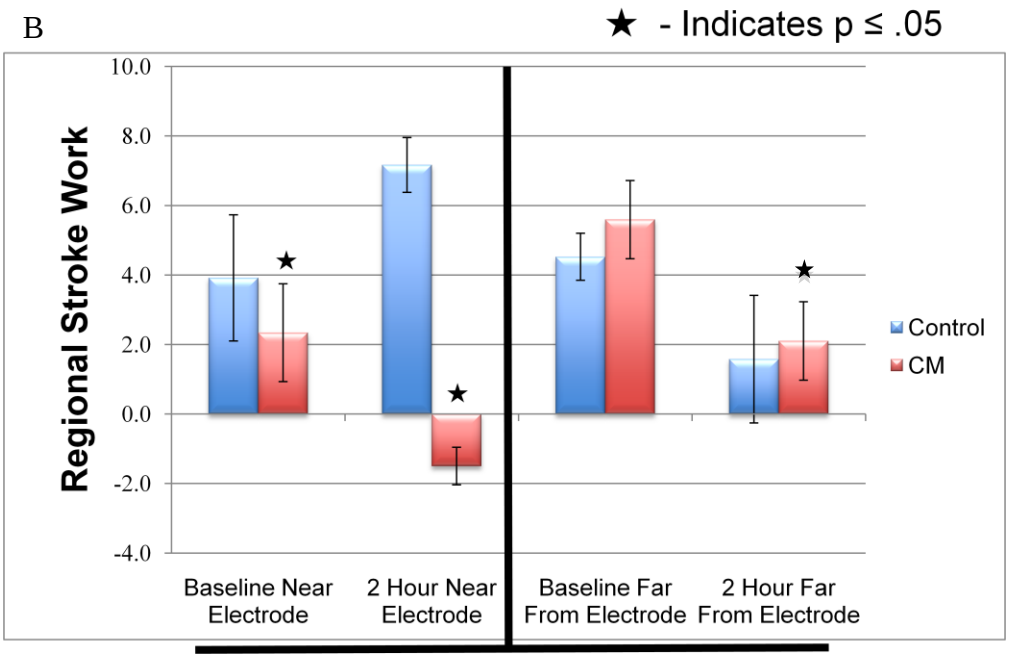

Figure 5.4: A) Schematic of sub-region of interest locations with respect to the pacing electrode. B) Regional stroke work in regions close to and far from the pacing electrode. There is a significant difference between baseline and after ventricular pacing upon return to normal activation pathways (atrial pacing) in the cardiac memory group.

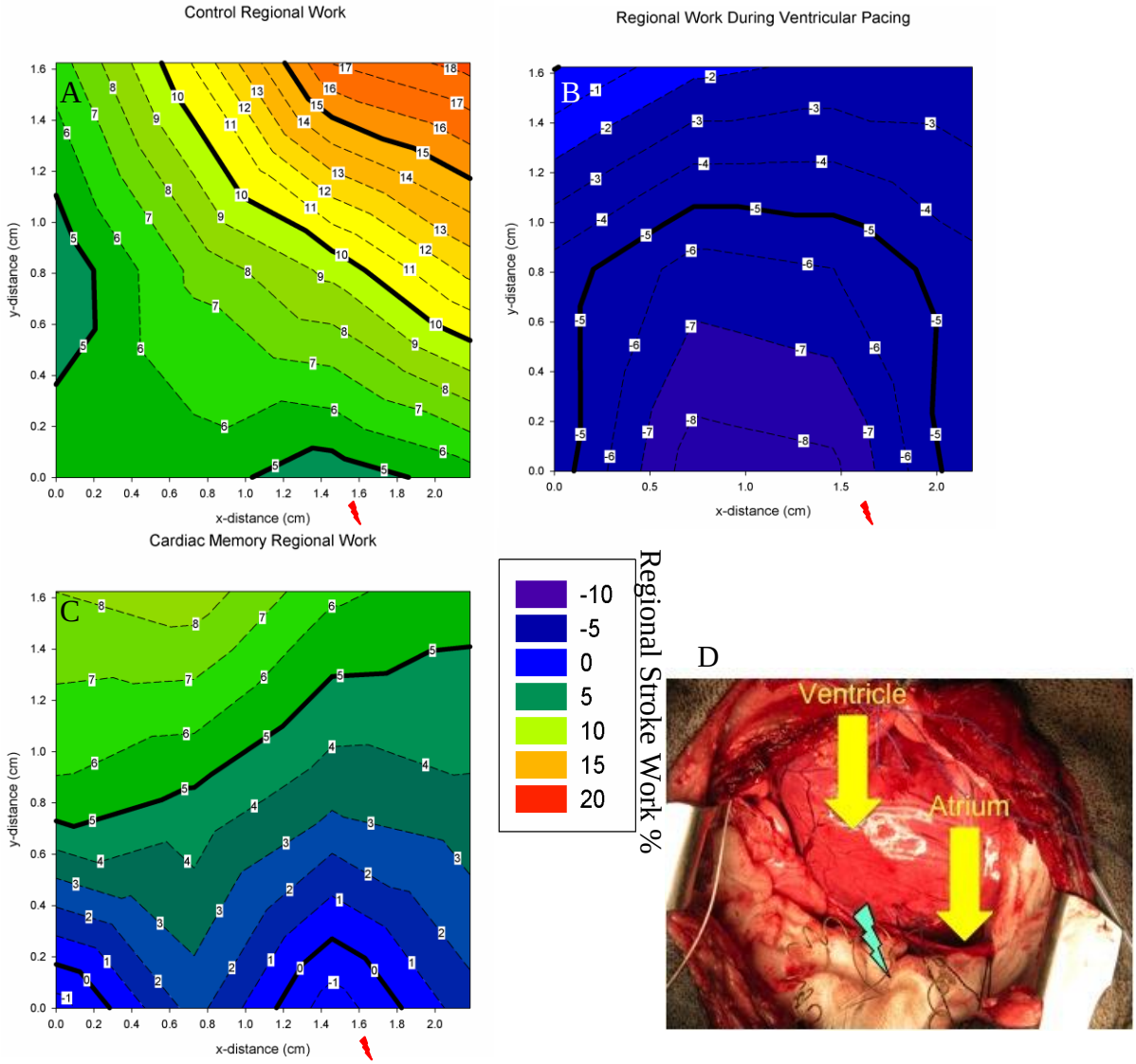

Figure 5.5: A) regional stroke work gradient after 2 hours of AP in control animal. B) regional stroke work gradient during VP in short term cardiac memory animal C) regional stroke work gradient after 2 hours of VP in short term cardiac memory animal D) Location of pacing electrode in the ventricle (atrium unexposed). Denotes pacing electrode location in panels A through C

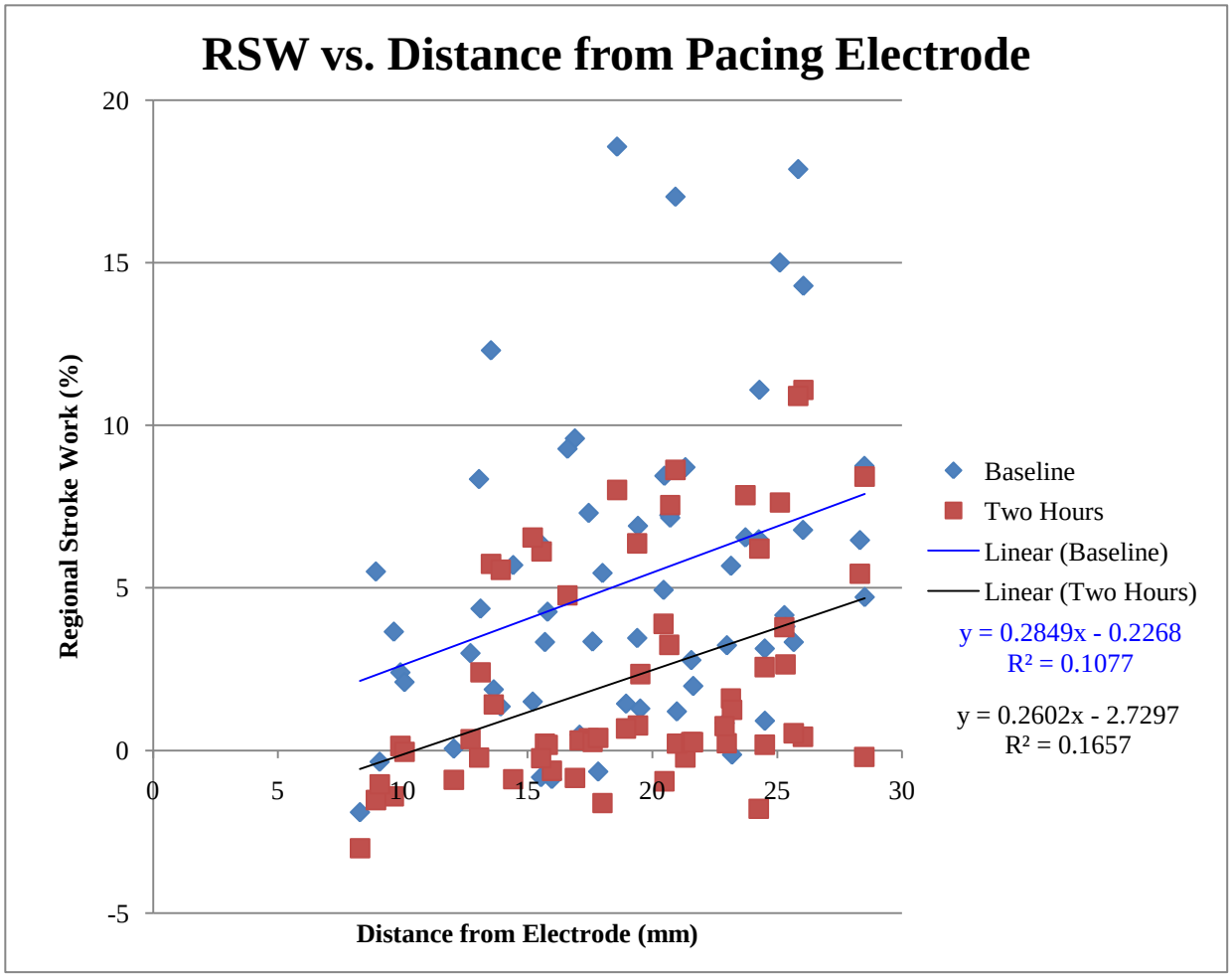

Figure 5.6: Scatter plot of regional stroke work vs. distance from pacing electrode. (Blue: Equation and correlation for baseline. Black: Equation and correlation for cardiac memory induced)

5.3 Specific Aim 2: Diastolic Twist

The camera axis was rotated to the heart axis by measuring the angle between the x-axis and the left anterior descending artery (LAD) via image correlation software. Each vector from the displacement matrices were rotated using Equation 14 to acquire rotated vector displacement matrices x' and y'. After rotating the vector displacement matrices diastolic twist was found. Baseline values of diastolic twist (-1.9 ± 0.4°) were not significantly different from those during ventricular pacing (-0.7 ± 0.8°) or after inducing cardiac memory (-2.2 ± 0.1°). In addition there was no significant difference between diastolic twist after inducing cardiac memory and during ventricular pacing. The diastolic twist rates also did not significantly differ at baseline (-23.1 ± 9.2 °/s) compared to ventricular pacing (-6.4 ± 7.1 °/s) or after inducing cardiac memory (-21.5 ± 1.9 °/s). Table 5-2 shows the average diastolic twist and rates.

Table 5-2: Diastolic twist and diastolic twist rate in cardiac memory animals at baseline (t=0), during ventricular pacing, and after two hours of ventricular pacing upon return to normal activation. Data (n=5): Mean ± SEM

	Baseline	VP	CM
Twist (°)	-1.9 ± 0.4	-0.7 ± 0.8	-2.2 ± 0.6
Rate (°/s)	-23.1 ± 9.2	-6.4 ± 7.1	-21.5 ± 1.9

5.4 Specific Aim 2: Systolic Principal Strain

Principal strains were calculated during systole for both the control group and the cardiac memory induced group by using the rotated x' and y' vector displacement matrices. Principal strains were measured in the control animals to determine if changes in principal strain occur without any treatment. After two hours of atrial pacing there was no significant difference in principal strain in the 1 direction (0.8 ±

1.2%) versus baseline (-0.7 ± 0.9%). Also there was no significant difference in principal strain in the 2 direction (-5.0 ± 2.0%) versus baseline (-6.0 ± 1.2%). Table 5-3 shows the principal strains in the 1 and 2 directions for control animals.

Principal strains in the 1 direction were found to be significantly different between baseline (-1.3 ± 0.5 %) and during ventricular pacing (5.2 ± 1.7 %)($p<0.05$). In addition, after inducing cardiac memory and returning to normal activation, principal strain in the 1 direction did not fully recover to baseline values (-0.3 ± 0.6 %)($p<0.05$) between both before pacing and during ventricular pacing). Conversely, principal strains in the 2 direction were found to be significantly different between baseline (-5.6 ± 0.9 %) and ventricular pacing (-1.6 ± 1.0 %)($p<0.05$), and between ventricular pacing and cardiac memory induced (-5.9 ± 0.7 %)($p<0.05$). Between baseline and cardiac memory there was no difference found for principal strain in the 2 direction. Table 5-4 shows principal strains in the 1 and 2 directions for cardiac memory induced animals.

Table 5-3: Control animal systolic principal strains at baseline (t=0) and after 2 hours of atrial pacing. Data: Mean ± SEM

	Baseline (n=4)	2 Hours (n=4)
Principal 1 (%)	-0.7 ± 0.9	0.8 ± 1.2
Principal 2 (%)	-6.0 ± 1.2	-5.0 ± 2.0

Table 5-4: Cardiac memory animal systolic principal strain results at baseline (t=0), during ventricular pacing, and after 2 hours of ventricular pacing upon return to normal activation pathways. Data: Mean ± SEM

	Baseline (n=5)	VP (n=5)	CM (n=5)
Principal 1 (%)	-1.3 ± 0.5	5.2 ± 1.7	-0.3 ± 0.6
Principal 2 (%)	-5.6 ± 0.9	-1.6 ± 1.0	-5.9 ± 0.7
	Baseline vs. CM	Baseline vs. VP	CM vs. VP
Principal 1	p=0.017	p=0.030	p=0.046
Principal 2	p=NS	p=0.026	p=0.011

6 *Discussion*

This project demonstrates a mechanical correlation to cardiac memory. The pacing protocol used induced short-term cardiac memory after two hours of pacing. The changes in regional stroke work, as well as systolic area contraction, after inducing cardiac memory were significantly different than baseline measurements. . Changes in regional stroke work and systolic area contraction remain after cessation of ventricular pacing upon return to normal activation pathways through atrial pacing show a mechanical cardiac memory. Further, during ventricular pacing both regional stroke work and systolic area contraction are significantly different than baseline.

Specific Aim 2 sought to determine if systolic or diastolic function change after inducing cardiac memory. Systolic function was measured through determination of principal strains. The results showed a significant change in the contractile principal strain after cessation of two hours of ventricular pacing. Diastolic function was measured through diastolic twist and diastolic twist rate. These results showed no significant change in diastolic function after inducing cardiac memory. This section discusses the significance of the results in terms of the goals of this project.

6.1 Global Function

Global function of the heart was measured through 4 parameters: tau, developed pressure, dP/dt_{max}, and dP/dt_{min}. Interestingly, tau, the isovolumic relaxation time constant for the heart, developed pressure, dP/dt_{max}, and dP/dt_{min}, did not change significantly with pacing or after inducing cardiac memory. This differs from

Heyndrickx et al. [51] who found that by increasing the heart rate through atrial pacing, tau was decreased while dP/dt_{max} and dP/dt_{min} increased. Further, they found that increasing the heart rate through ventricular pacing, tau and dP/dt_{max} decreased while dP/dt_{min} increased. Conversely Sorger et al.[34], through MRI tagging, saw no changes in developed pressure or in dP/dt_{min}, however measured a change in tau during ventricular pacing. The discrepancy in the results could be to different heart rates. Heyndrickx et al.[51] paced at 220 beats/min, while in this study the pacing rate was 150 beats/min. Much lower values for tau (18.2 ± 0.1 ms) were reported, while dP/dt_{max} (2560 ± 232 mmHg/s) and dP/dt_{min} (-2744 ± 158 mmHg/s) were similar. We report values of tau being 57.7 ± 7.3 during ventricular pacing. A possible source for the discrepancy could be a type II statistical error due to the small sample size.

6.2 Ventricular Pacing

Regional mechanical function during ventricular pacing was in agreement with other studies reported in the literature. Azeloglu et al.[3] measured regional stroke work and systolic area contraction in one ROI while changing pacing electrode location in the porcine heart and found regional stroke work in the region near the pacing electrode to be reduced from 8% during AP to 0 %. Herein, we report regional stroke work during ventricular pacing to be reduced from 6% to -4%, in close agreement to the other study. Azeloglu et al.[3] found an increase in regional stroke work with distance from the pacing electrode as well as a change in work with the pacing location around the region of interest.

6.3 Specific Aim 1: Mechanical Correlation to Cardiac Memory

Cardiac memory is defined as the persistent change in the T-wave, after a period of ventricular pacing, upon return to normal electrical activation. Altered ventricular activation induced by ventricular pacing, initiates altered contractile patterns and altered stretch, thus inducing cardiac memory[41]. The average regional stroke work decreased from 6.0 ± 3.3% prior to pacing to 2.4 ± 1.6% after cessation of two hours of ventricular pacing. Plotnikov et al.[37] induced short-term cardiac memory in canine models by two hours of ventricular pacing, whereas long-term cardiac memory was induced with 21 days of ventricular pacing. By administering drugs to the animals to block $I_{Ca(L)}$, they showed that $I_{Ca(L)}$ blockade prevents induction of both short term and long term cardiac memory. However administrating β-adrenergic blockers did not prevent induction of cardiac memory[37]. The L-Type calcium channel is a voltage-activated channel related to the accessory protein KChIP2. KChIP2 relates to the outward potassium current I_{to} that is related to the action potential duration. Changing the action potential duration will alter the contractility of the region and change the stretch. This relates to the area change of the region of interest. Regional stroke work is the discrete integration of pressure versus change in area. Therefore, changes seen in regional stroke work are resultant from the change in area of the myocardium.

Regional stroke work in regions closest to the pacing electrode had the greater changes compared to regions further away from the pacing electrode during VP and after returning to normal activation. Activation and stretch from altered activation was the greatest nearest the pacing electrode. Janse et al.[39] measured the

repolarization gradients in normal and cardiac memory induced canine models and showed that ventricular pacing for two hours and after returning to normal activation pathways decreased the repolarization times in the left ventricle by about 10 ms at 90% repolarization levels[39]. The change in repolarization times had an effect on the regional stroke work in those regions.

During AP the regional stroke work is positive across the entire region of interest ranging from 5% to almost 20% (Figure 5.5). Ventricular pacing changes the regional stroke work to be negative across the entire region of interest. Furthermore when atrial pacing is restored after two hours of ventricular pacing, the regional stroke work ranges from negative to positive, increasing with distance from the pacing site. This response is also seen during ventricular pacing. However, no consistent increase was seen with distance from the pacing electrode.

The protein cAMP response element binding (CREB) is a transcription factor that binds to cAMP response elements and has a possible involvement in heart failure. It essential to long term central nervous system memory and was therefore thought to be important to cardiac memory. Patberg et al.[7] measured CREB, using western blots, from biopsy punches, with distance from the pacing electrode in canine models during both short-term cardiac memory and long-term cardiac memory and showed CREB levels to decrease significantly from normal and a trend to increase with distance from the pacing electrode. Husse and Isenberg[52] showed that rats that were genetically modified to not express CREB developed dilated cardiomyopathy with decreased systolic and diastolic function[52]. Decreased systolic and diastolic

mechanical function remains after ventricular pacing, upon return to normal activation pathways (atrial pacing), suggesting a relationship between decreased mechanical function and decreased CREB levels as reported by Patberg et al.[7]

6.4 Specific Aim 2: Diastolic Twist

Torsion is the twisting of the heart due to an applied force in the circumferential direction. Torsion can be measured during diastole and is correlative to the global measure of the diastolic relaxation time constant or tau[21]. Dong et al.[21] used tagged MRI in canine models to measure the angular displacement of the base of the heart relative to the apex. The displacement angles were then transformed into torsion measurements and using maximum torsion and determined the recoil rates that were compared to the curve fit of tau during isovolumic relaxation. Herein we report diastolic twist and twist rate during atrial pacing was not significantly different than during ventricular pacing, or after inducing cardiac memory by two hours of ventricular pacing. Dong et al.[21] reported baseline relaxation rate to be 84° ± 38 (standard deviation), while herein reported baseline value of 23°± 9 is much lower. The heart rate could have an effect on this value, although Dong et al.[21] did not report heart rate.

6.5 Specific Aim 2: Systolic Principal Strain

Ventricular pacing or induction of cardiac memory changes the principal strain within the region of interest. The maximal principal strain, or elongation, decreases during ventricular pacing. However the minimal principal strain, or contraction, does

not change after inducing cardiac memory. The principal strain aligns with the orientation of the myocardial fibers. Delhaas et al.[2] measured the relation between regional electrical activation time and subepicardial fiber strain in the canine left ventricle using an optical method by tracking the movement of dots across the region of interest on the epicardial surface. Change in epicardial strain was reported during systole when pacing from the left ventricle. Prinzen et al.[9] measured circumferential wall strain in the canine heart, using MRI, and found a significant change in strain during systole due to ventricular pacing. Herein, only principal strain during systole was measured. Because systole is the contraction phase of the heart, in two dimensions any elongation is due to the Poisson effect (volume is conserved within an incompressible body, therefore if one direction contracts the other has to expand) and the elongation can be considered a conservation of volume. When comparing the principal strains the only motion caused by the myocytes is the contractile principal strain other strains are cell volume conservation.

There is a relation between systolic area contraction, stretch, and principal strains. Systolic area contraction is defined as the change in area between diastole and systole divided by the area at diastole or change in area during systole divided by initial area. Stretch is the maximal change in area divided by maximum area or the total amount of displacement a myocyte experiences during the cardiac cycle. Principal strain in the 1 direction and systolic area contraction are the maximal displacements a myocyte experiences during systole. Systolic area contraction and principal strains are measured during the same time, systole, whereas stretch is over the whole heartbeat.

Changes in principal strain near the pacing electrode after inducing cardiac memory indicate mechanical effects of cardiac memory. The principal strains are unchanged after two hours of atrial pacing, whereas ventricular pacing changes the principal strains and those changes did not return to previous levels after return to normal activation. Sosunov et al.[41] changed the stretch on an isolated rabbit heart by suturing pads to the epicardium and applying ~ 15% stretch and concluded that altered stretch is the ultimate determinant of cardiac memory. Principal strains herein, show a change in strain that equates to a change in stretch; thereby altering stretch and cardiac memory is induced. This change in stretch occurs during systole as shown by others. Yu et al.[46] used canine hearts to show the different ion currents involved in cardiac memory and concluded that $I_{to1,}$ present during phase 1 of the myocyte action potential (systole), was a significant factor in cardiac memory. Ricard et al.[43] performed experiments on isolated, perfused canine hearts to isolate stretch and demonstrate that ventricular pacing used to induce memory alters the contractile pattern of the left ventricle. Also studied were the effects of injecting angiotensin II receptor blockers, angiotensin-converting enzyme inhibitors and protease inhibitors, on inducing cardiac memory and concluded that alterations in myocardial stretch induced angiotensin II synthesis by cardiac cells. Finally there was a strong association between release of angiotensin II and occurrence of cardiac memory[43]. The data herein allows for determining stretch around the pacing site so that biopsies can be taken from the appropriate regions for optimal measurements.

7 Conclusions

Ventricular pacing for two hours decreases the mechanical function in the region closest to the pacing electrode. After pacing is returned to normal activation through the atrium, mechanical function remains depressed in regions close to the pacing electrode. Thus, similar to electrophysiological changes apparent in the T-wave, mechanical changes remain in the heart after pacing, suggesting a mechanical correlation to cardiac memory.

Cardiac memory could be either beneficial or detrimental to a person. If the arrhythmic event is remembered, the function could remain depressed due to cardiac memory. Conversely, it could be beneficial to correcting arrhythmias by developing pacing protocols to follow which will counteract the arrhythmic event and return the person to normal electrical activation pathways.

8 Future Studies

More studies are required to determine the root causes for cardiac memory. This includes further mechanical studies as well as protein analysis in regions of depressed mechanical function. Sonomicrometry measurements should be taken along with HDM in order to determine the volume of the heart. Using these measurements global function could be determined along with regional function. Regional and global studies for long-term cardiac memory should be performed to understand the difference between short term and long term cardiac memory.

Non-invasive studies (using MRI, ECHO, ect.) should be done to get global mechanics of the heart both during altered activation pathways and upon return to normal activation pathways. Using non-invasive techniques will eventually allow for characterization of cardiac memory in humans. This will ultimately be important in determining the best methods to use the knowledge gained from studying cardiac memory.

Finally studies should be done to relate electrical, mechanical and molecular changes during both short-term and long-term cardiac memory so that it is fully understood.

References

1. Lloyd-Jones D, Adams R, Carnethon M, De Simone G, Ferguson T, Flegal K, Ford E, Furie K, Go A, Greenlund K, Haase N, Hailpern S, Ho M, Howard V, Kissela B, Kittner S, Lackland D, Lisabeth L, Marelli A, McDermott M, Meigs J, Mozaffarian D, Nichol G, O'Donnell C, Roger V, Rosamond W, Sacco R, Sorlie P, Stafford R, Steinberger J, Thom T, Wasserthiel-Smoller S, Wong N, Wylie-Rosett J, Hong Y. Heart disease and stroke statistics--2009 update: a report from the American Heart Association Statistics Committee and Stroke Statistics Subcommittee. *Circulation.* 2009;119(3):480-486.

2. Delhaas T, Arts T, Prinzen F, Reneman R. Relation between regional electrical activation time and subepicardial fiber strain in the canine left ventricle. *Pflugers Arch.* 1993;423(1-2):78-87.

3. Azeloglu E, Yun Y, Saltman A, Krukenkamp I, Chiang F, Chen W, Gaudette G. High resolution mechanical function in the intact porcine heart: mechanical effects of pacemaker location. *J Biomech.* 2006;39(4):717-725.

4. Chatterjee K, Harris A, Davies J, Leatham A. T-wave changes after artificial pacing. *Lancet.* 1969;1(7598):759-760.

5. Rosenbaum M, Blanco H, Elizari M, Lázzari J, Davidenko J. Electrotonic modulation of the T wave and cardiac memory. *Am J Cardiol.* 1982;50(2):213-222.

6. Rosen M, Cohen I. Cardiac memory ... new insights into molecular mechanisms. *J Physiol.* 2006;570(Pt 2):209-218.

7. Patberg K, Plotnikov A, Quamina A, Gainullin R, Rybin A, Danilo PJ, Sun L, Rosen M. Cardiac memory is associated with decreased levels of the transcriptional factor CREB modulated by angiotensin II and calcium. *Circ Res.* 2003;93(5):472-478.

8. Shvilkin A, Danilo PJ, Wang J, Burkhoff D, Anyukhovsky E, Sosunov E, Hara M, Rosen M. Evolution and resolution of long-term cardiac memory. *Circulation.* 1998;97(18):1810-1817.

9. Prinzen F, Hunter W, Wyman B, McVeigh E. Mapping of regional myocardial strain and work during ventricular pacing: experimental study using magnetic resonance imaging tagging. *J Am Coll Cardiol.* 1999;33(6):1735-1742.

10. Wyman B, Hunter W, Prinzen F, Faris O, McVeigh E. Effects of single- and biventricular pacing on temporal and spatial dynamics of ventricular contraction. *Am J Physiol Heart Circ Physiol.* 2002;282(1):H372-379.

11. Berne RM. *Physiology*. 5th ed. St. Louis: Mosby; 2004.

12. Levy MN, Pappano AJ, Berne RM. *Cardiovascular physiology*. 9th ed. Philadelphia, PA: Mosby Elsevier; 2007.

13. Weiss J, Frederiksen J, Weisfeldt M. Hemodynamic determinants of the time-course of fall in canine left ventricular pressure. *J Clin Invest.* 1976;58(3):751-760.

14. Axel L, Dougherty L. Heart wall motion: improved method of spatial modulation of magnetization for MR imaging. *Radiology.* 1989;172(2):349-350.

15. Axel L, Dougherty L. MR imaging of motion with spatial modulation of magnetization. *Radiology.* 1989;171(3):841-845.

16. Kraitchman D, Wilke N, Hexeberg E, Jerosch-Herold M, Wang Y, Parrish T, Chang C, Zhang Y, Bache R, Axel L. Myocardial perfusion and function in dogs with moderate coronary stenosis. *Magn Reson Med.* 1996;35(5):771-780.

17. Kuijpers D, Ho K, van Dijkman P, Vliegenthart R, Oudkerk M. Dobutamine cardiovascular magnetic resonance for the detection of myocardial ischemia with the use of myocardial tagging. *Circulation.* 2003;107(12):1592-1597.

18. Young A, Kramer C, Ferrari V, Axel L, Reichek N. Three-dimensional left ventricular deformation in hypertrophic cardiomyopathy. *Circulation.* 1994;90(2):854-867.

19. Kramer C, Lima J, Reichek N, Ferrari V, Llaneras M, Palmon L, Yeh I, Tallant B, Axel L. Regional differences in function within noninfarcted myocardium during left ventricular remodeling. *Circulation.* 1993;88(3):1279-1288.

20. Notomi Y, Lysyansky P, Setser R, Shiota T, Popović Z, Martin-Miklovic M, Weaver J, Oryszak S, Greenberg N, White R, Thomas J. Measurement of ventricular torsion by two-dimensional ultrasound speckle tracking imaging. *J Am Coll Cardiol.* 2005;45(12):2034-2041.

21. Dong S, Hees P, Siu C, Weiss J, Shapiro E. MRI assessment of LV relaxation by untwisting rate: a new isovolumic phase measure of tau. *Am J Physiol Heart Circ Physiol.* 2001;281(5):H2002-2009.

22. Hankiewicz J, Lewandowski E. Improved cardiac tagging resolution at ultra-high magnetic field elucidates transmural differences in principal strain in the mouse heart and reduced stretch in dilated cardiomyopathy. *J Cardiovasc Magn Reson.* 2007;9(6):883-890.

23. Hankiewicz J, Goldspink P, Buttrick P, Lewandowski E. Principal strain changes precede ventricular wall thinning during transition to heart failure in a mouse model of dilated cardiomyopathy. *Am J Physiol Heart Circ Physiol.* 2008;294(1):H330-336.

24. Cupps B, Pomerantz B, Krock M, Villard J, Rogers J, Moazami N, Pasque M. Principal strain orientation in the normal human left ventricle. *Ann Thorac Surg.* 2005;79(4):1338-1343.

25. Brown LG. A survey of image registration techniques. *ACM Comput. Surv.* 1992;24(4):325-376.

26. Foroosh H, Zerubia J, Berthod M. Extension of phase correlation to subpixel registration. *IEEE Trans Image Process.* 2002;11(3):188-200.

27. Gaudette G, Todaro J, Krukenkamp I, Chiang F. Computer aided speckle interferometry: a technique for measuring deformation of the surface of the heart. *Ann Biomed Eng.* 2001;29(9):775-780.

28. Gaudette GR, Azeloglu EU, Oleszak L, Saltman AE, Krukenkamp IB, Chiang F-P. Determination of Regional Area Stroke Work With High Spatial Resolution in the Heart. *Cardiovasular Engineering.* 2002;2(4):129-137.

29. Gaudette G, Krukenkamp I, Azeloglu E, Saltman A, Lense M, Todaro J, Chiang F. Effects of ischemia on epicardial deformation in the passive rabbit heart. *J Biomech Eng.* 2004;126(1):70-75.

30. Kelly D, Azeloglu E, Kochupura P, Sharma G, Gaudette G. Accuracy and reproducibility of a subpixel extended phase correlation method to determine micron level displacements in the heart. *Med Eng Phys.* 2007;29(1):154-162.

31. Wood M, Ellenbogen K. Cardiology patient pages. Cardiac pacemakers from the patient's perspective. *Circulation.* 2002;105(18):2136-2138.

32. Simantirakis E, Vardakis K, Kochiadakis G, Manios E, Igoumenidis N, Brignole M, Vardas P. Left ventricular mechanics during right ventricular apical or left ventricular-based pacing in patients with chronic atrial fibrillation after atrioventricular junction ablation. *J Am Coll Cardiol.* 2004;43(6):1013-1018.

33. Sengupta P, Khandheria B, Korinek J, Jahangir A, Yoshifuku S, Milosevic I, Belohlavek M. Left ventricular isovolumic flow sequence during sinus and paced rhythms: new insights from use of high-resolution Doppler and ultrasonic digital particle imaging velocimetry. *J Am Coll Cardiol.* 2007;49(8):899-908.

34. Sorger J, Wyman B, Faris O, Hunter W, McVeigh E. Torsion of the left ventricle during pacing with MRI tagging. *J Cardiovasc Magn Reson.* 2003;5(4):521-530.

35. Kennedy RJ, Varriale P, Alfenito JC. *Textbook of vectorcardiography*. [1st ed. New York,: Medical Dept.; 1970.

36. del Balzo U, Rosen M. T wave changes persisting after ventricular pacing in canine heart are altered by 4-aminopyridine but not by lidocaine. Implications with respect to phenomenon of cardiac 'memory'. *Circulation.* 1992;85(4):1464-1472.

37. Plotnikov A, Yu H, Geller J, Gainullin R, Chandra P, Patberg K, Friezema S, Danilo PJ, Cohen I, Feinmark S, Rosen M. Role of L-type calcium channels in pacing-induced short-term and long-term cardiac memory in canine heart. *Circulation.* 2003;107(22):2844-2849.

38. Lee K, Chu C, Lin T, Yen H, Voon W, Sheu S, Lai W. Effect of sodium and calcium channel blockers on short-term cardiac memory in humans. *Int J Cardiol.* 2008;123(2):94-101.

39. Janse M, Sosunov E, Coronel R, Opthof T, Anyukhovsky E, de Bakker J, Plotnikov A, Shlapakova I, Danilo PJ, Tijssen J, Rosen M. Repolarization gradients in the canine left ventricle before and after induction of short-term cardiac memory. *Circulation.* 2005;112(12):1711-1718.

40. Ozgen N, Rosen M. Cardiac memory: a work in progress. *Heart Rhythm.* 2009;6(4):564-570.

41. Sosunov E, Anyukhovsky E, Rosen M. Altered ventricular stretch contributes to initiation of cardiac memory. *Heart Rhythm.* 2008;5(1):106-113.

42. Jeyaraj D, Wilson L, Zhong J, Flask C, Saffitz J, Deschênes I, Yu X, Rosenbaum D. Mechanoelectrical feedback as novel mechanism of cardiac electrical remodeling. *Circulation.* 2007;115(25):3145-3155.

43. Ricard P, Danilo PJ, Cohen I, Burkhoff D, Rosen M. A role for the renin-angiotensin system in the evolution of cardiac memory. *J Cardiovasc Electrophysiol.* 1999;10(4):545-551.

44. Coronel R, Opthof T, Plotnikov A, Wilms-Schopman F, Shlapakova I, Danilo PJ, Sosunov E, Anyukhovsky E, Janse M, Rosen M. Long-term cardiac memory in canine heart is associated with the evolution of a transmural repolarization gradient. *Cardiovasc Res.* 2007;74(3):416-425.

45. Yu H, Gao J, Wang H, Wymore R, Steinberg S, McKinnon D, Rosen M, Cohen I. Effects of the renin-angiotensin system on the current I(to) in epicardial and endocardial ventricular myocytes from the canine heart. *Circ Res.* 2000;86(10):1062-1068.

46. Yu H, McKinnon D, Dixon J, Gao J, Wymore R, Cohen I, Danilo PJ, Shvilkin A, Anyukhovsky E, Sosunov E, Hara M, Rosen M. Transient outward current, Ito1, is altered in cardiac memory. *Circulation.* 1999;99(14):1898-1905.

47. Patel P, Plotnikov A, Kanagaratnam P, Shvilkin A, Sheehan C, Xiong W, Danilo PJ, Rosen M, Peters N. Altering ventricular activation remodels gap junction distribution in canine heart. *J Cardiovasc Electrophysiol.* 2001;12(5):570-577.

48. Shyu K, Chen C, Wang B, Kuan P. Angiotensin II receptor antagonist blocks the expression of connexin43 induced by cyclical mechanical stretch in cultured neonatal rat cardiac myocytes. *J Mol Cell Cardiol.* 2001;33(4):691-698.

49. Dodge S, Beardslee M, Darrow B, Green K, Beyer E, Saffitz J. Effects of angiotensin II on expression of the gap junction channel protein connexin43 in neonatal rat ventricular myocytes. *J Am Coll Cardiol.* 1998;32(3):800-807.

50. Kochupura P, Azeloglu E, Kelly D, Doronin S, Badylak S, Krukenkamp I, Cohen I, Gaudette G. Tissue-engineered myocardial patch derived from extracellular matrix provides regional mechanical function. *Circulation.* 2005;112(9 Suppl):I144-149.

51. Heyndrickx G, Vantrimpont P, Rousseau M, Pouleur H. Effects of asynchrony on myocardial relaxation at rest and during exercise in conscious dogs. *Am J Physiol.* 1988;254(5 Pt 2):H817-822.

52. Husse B, Isenberg G. CREB expression in cardiac fibroblasts and CREM expression in ventricular myocytes. *Biochem Biophys Res Commun.* 2005;334(4):1260-1265.